

การพัฒนาแท่งระดับนาโนเมตรของทองคำทำให้เสถียรด้วยพอลิเมอร์ที่คอนจูเกตกับยา



นางสาวพิมพ์อร ชุนสุข

บทคัดย่อและแฟ้มข้อมูลฉบับเต็มของวิทยานิพนธ์ตั้งแต่ปีการศึกษา 2554 ที่ให้บริการในคลังปัญญาจุฬาฯ (CUIR)  
เป็นแฟ้มข้อมูลของนิสิตเจ้าของวิทยานิพนธ์ ที่ส่งผ่านทางบัณฑิตวิทยาลัย

The abstract and full text of theses from the academic year 2011 in Chulalongkorn University Intellectual Repository (CUIR)  
are the thesis authors' files submitted through the University Graduate School.

วิทยานิพนธ์นี้เป็นส่วนหนึ่งของการศึกษาตามหลักสูตรปริญญาวิทยาศาสตรมหาบัณฑิต

สาขาวิชาเคมี ภาควิชาเคมี

คณะวิทยาศาสตร์ จุฬาลงกรณ์มหาวิทยาลัย

ปีการศึกษา 2558

ลิขสิทธิ์ของจุฬาลงกรณ์มหาวิทยาลัย

DEVELOPMENT OF GOLD NANORODS STABILIZED WITH DRUG-CONJUGATED POLYMER

Miss Phim-on Khunsuk



A Thesis Submitted in Partial Fulfillment of the Requirements  
for the Degree of Master of Science Program in Chemistry

Department of Chemistry

Faculty of Science

Chulalongkorn University

Academic Year 2015

Copyright of Chulalongkorn University



พิมพ์อร ชุนสุข : การพัฒนาแท่งระดับนาโนเมตรของทองคำทำให้เสถียรด้วยพอลิเมอร์ที่  
คอนจูเกตกับยา (DEVELOPMENT OF GOLD NANORODS STABILIZED WITH DRUG-  
CONJUGATED POLYMER) อ.ที่ปริกษาวิทยานิพนธ์หลัก: รศ. ดร.วรวีร์ โฮเว่น, 49 หน้า.

ใช้ประโยชน์จากการที่อนุภาคระดับนาโนเมตรของทองคำ (gold nanorods; AuNRs) ออก  
ฤทธิ์แบบเสริมกัน สำหรับการบำบัดรักษามะเร็งทั้งจากการใช้ความร้อนและเคมีบำบัด ประกอบการมี  
สมบัติแปรเปลี่ยนได้ตามสารที่ทำให้เสถียร งานวิจัยนี้จึงสนใจที่จะพัฒนาอนุภาคระดับนาโนเมตรของ  
ทองคำ ที่ทำให้เสถียรด้วยโคพอลิเมอร์แบบสุ่มชนิด poly[(methacrylic acid)-*ran*-  
(methacryloyloxyethyl phosphorylcholine)] (PMAMPC) เป็นพาหะในการนำส่งยาบำบัดรักษา  
มะเร็ง โดยทำการคอนจูเกตยารักษามะเร็ง Doxorubicin (DOX) ไปยัง PMAMPC ผ่านการเกิดพันธะ  
ไฮโดรเจนซึ่งถูกทำลายได้ง่ายภายใต้สภาวะที่เป็นกรดในไลโซโซม จากนั้นเคลือบพื้นผิวของ AuNRs  
ด้วยโคพอลิเมอร์ที่คอนจูเกตกับ DOX (PMAMPC-DOX) ผ่านการเกิดพันธะ Au-S จากผลการทดลอง  
พบว่า PMAMPC-DOX-AuNRs มีเสถียรภาพที่ดีและมีขนาดที่ใกล้เคียงกัน จากการศึกษาการ  
ปลดปล่อยยาในหลอดทดลองพบว่า PMAMPC-DOX สามารถปลดปล่อย DOX ออกมามากขึ้นที่ pH  
5.0 และยืนยันการเข้าเซลล์ของ DOX ที่ถูกกระตุ้นให้ปลดปล่อยออกมาในสภาวะกรดภายใน  
เซลล์มะเร็งได้ด้วยเทคนิค confocal laser scanning microscopy นอกจากนี้จากการศึกษาพบว่า  
การบำบัดด้วยความร้อนร่วมกับเคมีบำบัดโดยใช้ PMAMPC-DOX-AuNRs มีประสิทธิภาพในการ  
ทำลายเซลล์มะเร็งมีมากกว่าการใช้วิธีใดวิธีหนึ่งเพียงอย่างเดียว ซึ่งจากผลการทดลองดังกล่าวแสดงให้เห็น  
เห็นว่า PMAMPC-DOX-AuNRs มีศักยภาพในการนำไปประยุกต์เป็นพาหะในการนำส่งยาที่กระตุ้น  
ด้วยกรดสำหรับการรักษามะเร็งแบบเสริมกัน

ภาควิชา เคมี

ลายมือชื่อนิสิต .....

สาขาวิชา เคมี

ลายมือชื่อ อ.ที่ปริกษาหลัก .....

ปีการศึกษา 2558

# # 5672039323 : MAJOR CHEMISTRY

KEYWORDS: SYNERGISTIC THERAPY / DRUG-CONJUGATED POLYMER / BIOCOMPATIBLE GOLD NANORODS / ACID-LABILE HYDRAZONE LINKAGE / METHACRYLOYLOXYETHYL PHOSPHORYLCHOLINE / RAFT POLYMERIZATION

PHIM-ON KHUNSUK: DEVELOPMENT OF GOLD NANORODS STABILIZED WITH DRUG-CONJUGATED POLYMER. ADVISOR: ASSOC. PROF. VORAVEE HOVEN, Ph.D., 49 pp.

Taking advantages of gold nanorod (AuNRs) being capable of providing synergistic efficiency for cancer treatment via the combination of photothermal therapy and chemotherapy and their tunable properties as a function of stabilizer, this work aims to develop anticancer drug delivery system based on AuNRs stabilized with poly[(methacrylic acid)-*ran*-(methacryloyloxyethyl phosphorylcholine)] (PMAMPC). Doxorubicin (DOX), an anticancer drug was conjugated to PMAMPC by acid-labile hydrazone linkage which should be rapidly destroyed under acidic environment in lysosomes. The DOX-conjugated PMAMPC (PMAMPC-DOX) was coated on AuNRs surface via Au-S bonds. The resulting PMAMPC-DOX-AuNRs showed good colloidal stability and uniform size. *In vitro* drug release studies demonstrated that DOX release can be significantly accelerated at pH 5.0. The efficient intracellular acid-triggered DOX release inside of cancer cells was confirmed using confocal laser scanning microscopy analysis. Furthermore, the combined photothermal-chemo treatment of cancer cells using PMAMPC-DOX-AuNR exhibited higher therapeutic efficacy than either single treatment alone. These results suggested that PMAMPC-DOX-AuNRs could potentially be applied in pH-triggered drug delivery for synergistic cancer therapy.

Department: Chemistry

Student's Signature .....

Field of Study: Chemistry

Advisor's Signature .....

Academic Year: 2015

## ACKNOWLEDGEMENTS

First of all, I would like to thank and express my heartfelt gratitude and appreciation to my advisor, Associate Professor Voravee Hoven for invaluable suggestion, guidance, constructive criticism, encouragement and kindness throughout the course of this research. I wish to deeply thank the thesis committee: Associate Professor Vudhichai Parasuk, Associate Professor Nongnuj Muangsin and Dr. Warayuth Sajomsang for reviewing my thesis and making valuable suggestion and critical comments.

I owe a deep sense of gratitude to Associate Professor Tanapat Palaga from Department of Microbiology, Faculty of Science and Interdisciplinary Program in Medical Microbiology, Chulalongkorn University for collaboration, valuable guidance, keen interest and timely suggestion throughout my research period.

Financial support for this work was provided by the Thailand Research Fund (DBG5580003) and Ratchadapiseksomphot Endowment Fund under Outstanding Research Performance Program (GF\_58\_08\_23\_01). PK acknowledges the Development and Promotion of Science and Technology Talents Project (DPST) for a M.Sc. scholarship.

Special thanks are extended to Supattra Chawalitpong from department of Biotechnology and Pritsana Sawutdeechaikul from department of Microbiology, Faculty science, Chulalongkorn University for assistance in cells studies, their kind help and co-operation.

Moreover, I am extremely thankful to all members of VH and VT group in Organic Synthesis Research Unit (OSRU) of Chulalongkorn University, for their friendship, assistance and suggestion concerning experimental techniques during my thesis work.

Finally, I also wish to especially thank my family for their love, kindness and support throughout my entire study.

## CONTENTS

	Page
THAI ABSTRACT .....	iv
ENGLISH ABSTRACT .....	v
ACKNOWLEDGEMENTS .....	vi
CONTENTS .....	vii
LIST OF FIGURES .....	x
LIST OF TABLES .....	xiii
LIST OF SCHEMES .....	xiv
LIST OF ABBREVIATION.....	xv
CHAPTER I INTRODUCTION.....	1
1.1 Introduction .....	1
1.2 Objectives.....	10
1.3 Scope of investigation.....	10
CHAPTER II MATERIALS AND METHODS .....	12
2.1 Materials .....	12
2.2 Characterization .....	12
2.3 Preparation of PMAMPC-DOX-AuNRs .....	13
2.3.1) Synthesis of PMAMPC by RAFT polymerization .....	13
2.3.2) Synthesis of Thiol-terminated PMAMPC (PMAMPC-SH) .....	14
2.3.3) Modification of PMAMPC-SH with Cysteamine.....	15
2.3.4) Modification of PMAMPC-Cys with Hydrazine.....	15
2.3.5) Conjugation of Doxorubicin.....	16
2.3.6) Synthesis of AuNRs by Seed-mediated Growth method .....	16

	Page
2.3.7)Preparation of Polymer-stabilized AuNRs via Ligand Exchange .....	17
2.3.8)Determination of the DOX loading content on AuNRs by Cyanide Digestion .....	18
2.4 <i>In vitro</i> Drug Release Studies.....	18
2.5 <i>In vitro</i> Photothermal Studies .....	18
2.6 Cell culture .....	19
2.7 <i>In vitro</i> Cytotoxicity Assay .....	19
2.8 Cellular Uptake Study.....	20
2.9 <i>In vitro</i> Synergistic Therapy.....	20
CHAPTER III RESULTS AND DISCUSSION.....	22
3.1 Preparation and Characterization of PMAMPC-DOX-AuNRs.....	22
3.1.1)Preparation of PMAMPC and Thiol-Terminated PMAMPC (PMAMPC-SH)..	22
3.1.2)Modification of PMAMPC-SH and Doxorubicin Conjugation.....	24
3.1.3)Synthesis of AuNRs by Seed-mediated Growth Method (CTAB-AuNRs)....	27
3.1.4)Preparation of Polymer-stabilized AuNRs via Ligand Exchange .....	28
3.1.5)Determination of the DOX Loading Content of AuNRs by Cyanide Digestion .....	31
3.2 <i>In vitro</i> Drug Release Studies.....	32
3.3 <i>In vitro</i> Photothermal Studies .....	33
3.4 <i>In vitro</i> Cytotoxicity Assay .....	34
3.5 Cellular Uptake Study.....	35
3.6 <i>In vitro</i> Synergistic Therapy.....	38
CHAPTER IV CONCLUSION AND SUGGESTION.....	41
REFERENCES .....	43



	Page
APPENDIX.....	46
VITA.....	49



## LIST OF FIGURES

Figure	Page
<b>Figure 1.1</b> AuNRs in different aspect ratios [1].....	2
<b>Figure 1.2</b> Schematics of (A) CTAB bilayer-capped AuNRs, (B) functionalized AuNRs with the CTAB bilayer completely exchanged, (C) functionalized AuNRs with the CTAB bilayer partially exchanged, and (D) secondarily functionalized AuNRs [11]. .....	2
<b>Figure 1.3</b> Schematic representation of PAA-coating procedure of AuNRs using PAA and subsequent bio-functionalization to prepare molecular probes for cellular labeling [8]. .....	3
<b>Figure 1.4</b> A schematic illustration of the multifunctional DOX-cRGD-AuNRs drug delivery and PET imaging [5]. .....	5
<b>Figure 1.5</b> A schematic illustration of the PEG-DOX-PAMAM-AuNRs for combined photothermal-chemo therapy [13]. .....	6
<b>Figure 1.6</b> schematic illustration of AuNRs coated with poly(MPC-co-DHLA) for nonfouling surface [18]. .....	7
<b>Figure 1.7</b> (i) Structure of PMPC-DOX and (ii) survival curve for mice treated with PMAMPC-DOX [19]. .....	8
<b>Figure 1.8</b> The mechanism of RAFT polymerization[20]. .....	9
<b>Figure 1.9</b> Schematic illustration of AuNRs stabilized with DOX-conjugated PMAMPC (PMAMPC-DOX-AuNRs) for synergistic cancer therapy. ....	10
<b>Figure 2.1</b> Schematic illustration of ligand exchange process. ....	17
<b>Figure 3.1</b> <sup>1</sup> H NMR spectra of PMAMPC (i) and PMAMPC-SH (ii) in D <sub>2</sub> O. ....	23
<b>Figure 3.2</b> UV-vis absorption spectra of PMAMPC DP100 (MA:MPC = 50:50) before (—) and after (---) reduction. ....	24
<b>Figure 3.3</b> FTIR spectra of (i) PMAMPC-SH, (ii) PMAMPC-Cys, (iii) PMAMPC-Cys-Hy, (iv) PMAMPC-DOX, and (v) DOX .....	26

<b>Figure 3.4</b> UV-Vis absorption spectra of PMAMPC-DOX in Milli-Q water .....	27
<b>Figure 3.5</b> (i) UV-Vis absorption spectra of CTAB-AuNRs prepared by seed-mediated growth method and (ii) TEM image of CTAB-AuNRs (scale bar 20 nm) .....	28
<b>Figure 3.6</b> UV-Vis absorption spectra of PMAMPC- AuNRs suspension in 10 mM PBS having varied MA:MPC composition; 78:22 (— —), 50:50 (— —), 29:71 (— —), and CTAB-AuNRs (.....).....	29
<b>Figure 3.7</b> UV-vis absorption spectra of CTAB-AuNRs (—), PMAMPC-Cys-AuNRs (—) and PMAMPC-DOX-AuNRs (—) suspension in 10 mM PBS .....	30
<b>Figure 3.8</b> UV-vis absorption spectra of PMAMPC-DOX-AuNRs before (—) and after (—) digestion and PMAMPC-Cys-AuNRs before (—) and after (.....) digestion. ....	32
<b>Figure 3.9</b> <i>In vitro</i> drug release measurement of PMAMPC-DOX-AuNRs DOX release profile from PMAMPC-DOX in pH 5.0 (dot point) and pH 7.4 (square point) buffers .....	33
<b>Figure 3.10</b> Temperature change of PMAMPC-DOX-AuNRs aqueous solutions having varied Au element concentrations (0 -10 $\mu\text{g/mL}$ ) during NIR laser irradiation for up to 15 min. ....	34
<b>Figure 3.11</b> Cell viability (%) of MDA-MB-231 cells after incubation with increasing concentration of compound as determined by MTS assay: (i) PMAMPC-Cys-AuNRs, (ii) PMAMPC-DOX-AuNRs, (iii) DOX and (iv) CTAB-AuNRs. Error bars represent absorbance variability measured at 492 nm where n=3.....	35
<b>Figure 3.12</b> CLSM analysis of intracellular DOX release from PMAMPC-DOX-AuNRs in comparison with DOX and PMAMPC-DOX. MDA-MB-231 cells were treated with PMAMPC-DOX-AuNRs having 15 $\mu\text{g/mL}$ of DOX for 30 min, followed by CLSM observation with time; blue fluorescence: nucleus staining dry, DAPI; red fluorescence: DOX; scale bar = 50 $\mu\text{m}$ . ....	37
<b>Figure 3.13</b> CLSM analysis of intracellular DOX release from PMAMPC-DOX-AuNRs. MDA-MB-231 cells were treated with PMAMPC-DOX-AuNRs having 15 $\mu\text{g/mL}$ of	

DOX for 2 h, followed by CLSM observation with time; blue fluorescence: DAPI;  
red fluorescence: DOX; scale bar: 50  $\mu\text{m}$ ..... 38

**Figure 3.14** *In vitro* synergistic therapy of PMAMPC-DOX-AuNRs. *In vitro*  
cytotoxicity of PMAMPC-DOX-AuNRs (blue column), PMAMPC-Cys-AuNRs (red  
column) and free DOX (yellow column) having Au element concentration = 5  
 $\mu\text{g/mL}$  against MDA-MB-231 cells by MTS assay at various irradiation time. .... 39

**Figure A1**  $^1\text{H}$  NMR spectrum of PMAMPC in  $\text{D}_2\text{O}$ ..... 47

**Figure A2** DOX calibration curve measured in Milli-Q water..... 48



## LIST OF TABLES

Table	Page
<b>Table 2.1</b> Varied amount of MA and MPC monomer for RAFT polymerization varied MA:MPC component.....	14
<b>Table 3.1</b> Summary of composition and molecular weight of PMAMPC copolymer .	23
<b>Table 3.2</b> Morphology information of the developed AuNRs.....	31



## LIST OF SCHEMES

Schemes	Page
<b>Scheme 3.1</b> Synthetic route employed for the preparation of PMAMPC-DOX.....	25
<b>Scheme 3.2</b> pH-sensitive DOX release behavior of PMAMPC-DOX.....	33



## LIST OF ABBREVIATION

ACVA	: 4,4'-Azobis(4-cyanovaleric acid)
AuNRs	: Gold nanorods
CPD	: 4-Cyano-4-(thiobenzoylthio)pentanoic acid
Cys	: Cysteamine
DOX	: Doxorubicin
EDC	: 1-Ethyl-3-(3-dimethylaminopropyl)carbodiimide
FTIR	: Fourier-Transform Infrared Spectroscopy
Hy	: Hydrazine
NHS	: <i>N</i> -hydroxysuccinimide
PBS	: Phosphate buffered saline
PMAMPC	: Poly[(methacrylic acid)- <i>ran</i> -(2-methacryloyloxyethyl phosphorylcholine)]
RAFT	: Reversible addition-fragmentation chain transfer
TEM	: Transmission electron microscope

# CHAPTER I

## INTRODUCTION

### 1.1 Introduction

Various classes of nanoparticles (physical size ~1-100 nm) have been developed for drug delivery and cancer cell diagnostics such as organic materials (e.g. polymers, dendrimers, and solid lipid) and inorganic materials (e.g. magnetic iron oxide, quantum dots of diverse mineral contents, silver, gold, and silica) [1-4]. Besides having high surface area like many nanocarriers, gold nanoparticles (AuNPs) exhibit additional favorable characteristics such as enhanced permeability and retention effects (EPR). They also possess unique optical properties with surface plasmon characteristics [1, 5]. Their cytotoxicity are lower than other nanomaterials such as semiconductors and metal oxide [6].

Specifically, elongated spherical gold nanoparticles or gold nanorods (AuNRs) can be taken up into cells more efficiently than spherical particles [7] and are known to exhibit longitudinal surface plasmon resonance (SPR) absorption in near-infrared (NIR) region depending on their size and shape (**Figure 1.1**), they occupy attractive optical properties and unique application potentials especially in photothermal therapy [8], molecular imaging [9] and gene therapy [6]. Once the AuNRs are applied as carriers for photothermal therapy, during NIR irradiation into the longitudinal SPR bands, the excited conduction band electrons decay to the ground state by releasing their energy as heat to the local environment. In other words, they can convert the absorbed light to heat called “photothermal effect” [1, 10] considering that NIR irradiation in the 800-1100 nm region can deeply and non-invasively penetrate into tissues with minimal skin absorption [6].



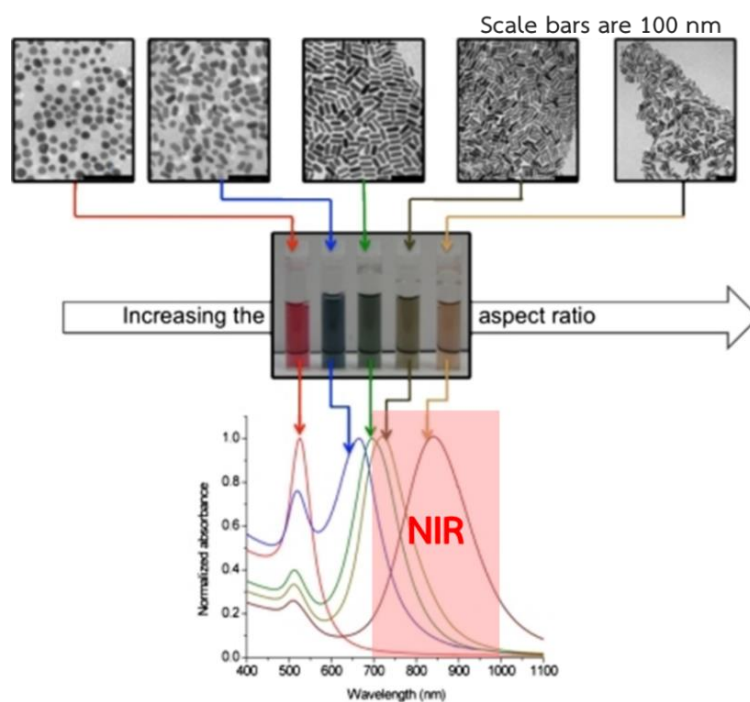


**Figure 1.1** AuNRs in different aspect ratios [1].

However, toxicity arisen from the cetyltrimethylammonium bromide (CTAB) used as templates for AuNPs synthesis limits their biomedical application, therefore it is necessary to develop AuNRs coated with water soluble and biocompatible molecule which are appropriate when they are applied in body system. This can be achieved by adsorbing such molecules on CTAB bilayer (**Figure 1.2D**) or exchange bilayer CTAB partially or completely with such molecules functionalized with thiol functionality (**Figure 1.2B-C**).

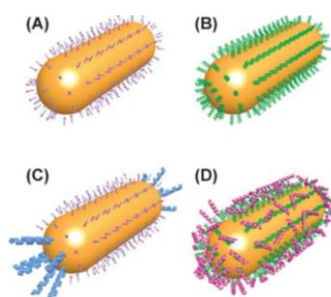


**Figure 1.2** Schematics of (A) CTAB bilayer-capped AuNRs, (B) functionalized AuNRs with the CTAB bilayer completely exchanged, (C) functionalized AuNRs with the CTAB bilayer partially exchanged, and (D) secondarily functionalized AuNRs [11].

In 2011, Kirui, *et al.* [8] modified AuNRs surface as secondary functionalized AuNRs (similar to what has been shown in **Figure 1.2D**) by direct coating of CTAB-stabilized AuNRs with poly(acrylic acid) (PAA) through simple electrostatic adsorption between negatively charges of PAA to positively charges of CTAB resulting in rods with carboxyl groups for attachment of targeting agents for colorectal cancer cells, A33scFv, as shown in **Figure 1.3**. The PAA-coated AuNRs showed good colloidal stability and selective photothermal therapy as demonstrated by more than 62% cell death being observed after cells were treated with A33scFv-AuNRs upon NIR irradiation.

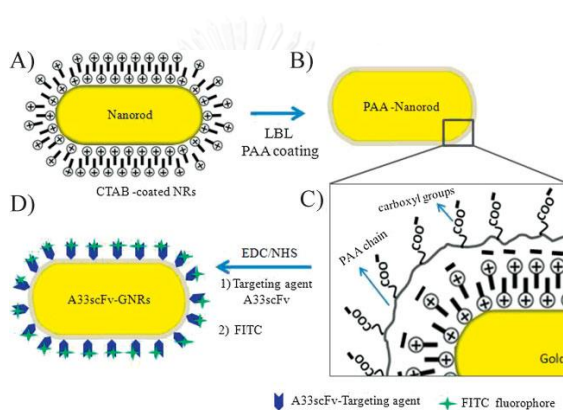


**Figure 1.3** Schematic representation of PAA-coating procedure of AuNRs using PAA and subsequent bio-functionalization to prepare molecular probes for cellular labeling [8].

Although coating biocompatible polymer via electrostatic interactions can reduce the cytotoxicity, CTAB still remained between AuNRs surface and the coated polymer. Another way is functionalization of AuNRs with biocompatible molecule through gold-thiol bonding (Au-S) chemistry via ligand exchange process which should be better routes to reduce the toxicity originated from CTAB on AuNRs surface for completely or partially functionalizing the surface of AuNRs (**Figure 1.2B** and C). High molecular weights of large thiol-terminated polymers, such as poly(ethylene glycol)s (PEGs) [5, 10, 12] and DNAs [6], have been employed to provide steric stabilization to the AuNRs. They are superior to small thiol molecules which often lead to aggregation of AuNRs [11]. From the research of Liao and Hafner in 2005 [12], thiol-terminated PEGs was coated onto AuNRs surface yielding PEGylated AuNRs with high stabilities and

biocompatibilities. From Raman spectroscopy, they found the absence of CTAB on the PEGylated AuNRs suggesting that PEGs can completely replace the CTAB bilayer on AuNRs surface.

Conjugating the designated polymer with some anticancer drug, polymer-coated AuNRs are capable of providing synergistic effect for cancer treatment via the combination of photothermal therapy and chemotherapy. Doxorubicin (DOX) is a model anticancer drug commonly used in the treatment of a wide range of cancers[4]. However, there are a number of drawbacks such as dose limiting toxicity, short circulation time and low water solubility that limit its efficiency in cancer treatment. To overcome such limitation, a number of researchers have tried to directly conjugate DOX onto AuNRs surface especially via acid-labile hydrazone linkage [5, 13, 14] because the tumor tissue environment is usually more acidic (pH 6.5) than blood and normal tissues (pH 7.4), and the pH value of endosome and lysosome within the cells are even lower at  $\sim 5.5$ – $6.0$  and  $\sim 4.5$ – $5.0$ , respectively [14, 15]. So by using this concept, pH-triggered drug delivery system can be developed from AuNRs for cancer therapy.

In 2012, Xiao, *et al.* [5] developed AuNRs as multifunctional drug carriers by conjugating DOX via acid-labile hydrazone linkage onto PEGylated AuNRs for chemo-effect and attachment of targeting molecule; cyclo(Arg-Gly-Asp-D-Phe-Cys) peptides (cRGD) and  $^{64}\text{Cu}$ -chelators (1,4,7-triazacyclononane-*N*, *N'*, *N''*-triacetic acid (NOTA)) for positron emission tomography (PET) imaging (**Figure 1.4**). *In vitro* studies found that the developed AuNRs showed good water solubility, drug release in acid environment and reduction of drug indiscrimination.

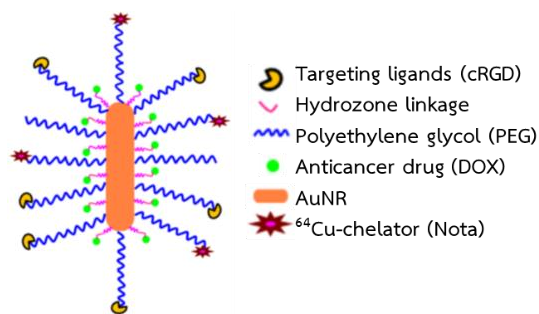


**Figure 1.4** A schematic illustration of the multifunctional DOX-cRGD-AuNRs drug delivery and PET imaging [5].

In 2014, Li, *et al.* [13] synthesized AuNRs stabilized by CTAB and replaced CTAB on AuNRs surface with poly(ethylene glycol)-attached PAMAM G4 dendrimers (PEG-PAMAM) then conjugated with DOX by acid-labile hydrazone linkage which should be rapidly destroyed under acidic environment (i.e. endo/lysosome) as shown in **Figure 1.5**. PEG-DOX-PAMAM-AuNRs had excellent colloidal stability and low cytotoxicity. *In vitro* drug release studies verified that DOX was negligibly released from the particles under pH 7.4, but it was enhanced significantly in acidic buffer (pH 5.0) with 88.2% drug release by 60 h. Intracellular pH-triggered DOX release behavior in lysosomes was confirmed by confocal laser scanning microscopy. Moreover, *in vitro* and *in vivo* combined photothermal-chemo treatment of cancer cells exhibited more effective therapeutic potency than either single treatment alone, suggesting that combination of photothermal process with chemotherapy provided synergistic effect on cancer cell damaging, thus enhancing efficiency of cancer therapy.

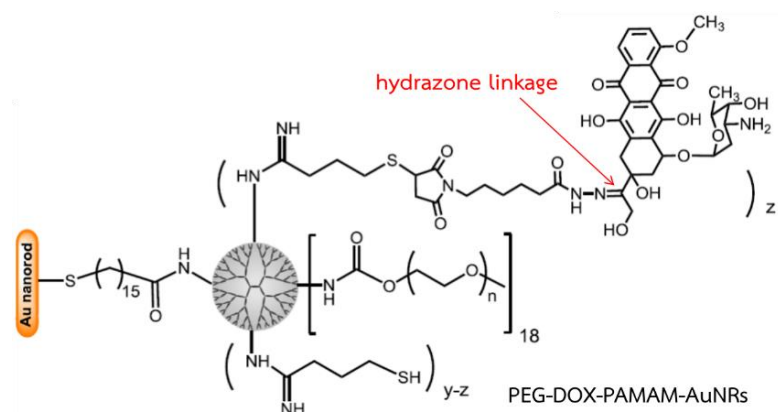


**Figure 1.5** A schematic illustration of the PEG-DOX-PAMAM-AuNRs for combined photothermal-chemo therapy [13].

In general, non-specific adsorption often occurs when drug carriers journey in body. It is quite a common practice to incorporate antifouling characteristic to the carriers. Poly(methacryloyloxyethyl phosphorylcholine) (PMPC) with cell-membrane mimic structure is one of well-known zwitterionic polymers that has been used for preparing nonfouling materials [16, 17] including AuNRs[18]. Recently, Chen, *et al.* [18] succeeded in preparing nonfouling AuNRs by ligand exchanging the CTAB bilayer on AuNRs surface with poly(2-methacryloyloxyethyl phosphorylcholine-co-dihydrolipoic acid) (poly(MPC-co-DHLA)) (as shown in **Figure 1.6**) which were synthesized by reversible addition-fragmentation chain transfer (RAFT) polymerization of MPC and the methacrylate of lipoic acid (LA), followed by reduction of the disulfides to give dihydrolipoic acid (DHLA) pendent groups. AuNRs coated with poly(MPC-co-DHLA) showed good colloidal stability, and resisted cyanide ion digestion because numerous thiol-terminated groups in each copolymer chain allowed them to efficiently bound on AuNRs surface. Due to their surface coating, the particle also showed nonfouling properties and noncytotoxicity to cancer and non-cancer cells.

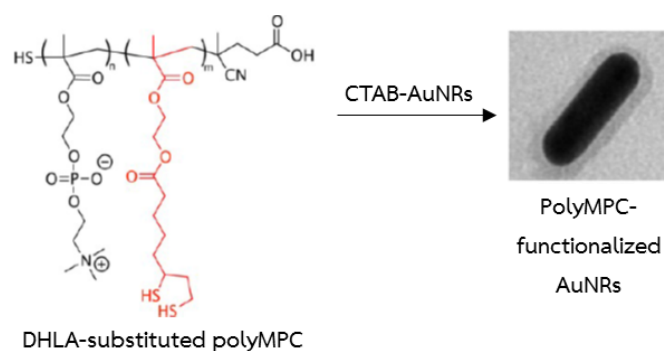


**Figure 1.6** schematic illustration of AuNRs coated with poly(MPC-co-DHLA) for nonfouling surface [18].

In addition, Page, et al. [19] have demonstrated that copolymer having PMPC, poly[(2-methacryloyloxyethyl phosphorylcholine)-*ran*-(2-ethoxy-2-oxoethyl methacrylate)] (poly(MPC-EtOEMA)) has also been employed to generate polymeric drug by conjugating DOX with EtOEMA unit via acid-labile hydrazone linkage (**Figure 1.7, i**) with the DOX loading of 22 wt %. PMPC-DOX conjugates exhibited pH sensitive release behavior and their maximum tolerated dose were about 30–50 mg/kg (DOX equivalent) in healthy mice. Conjugating DOX in PMPC prolonged the circulation in mice model with 8 times better than that of the free drug. Moreover, they demonstrate the efficiency of PMPC-DOX in 4T1 tumor-bearing mice for breast cancer treatment that overall survival in the PMPC-DOX group extended almost 2-fold (29 days) compared to both the untreated and free DOX treated mice as shown in **Figure 1.7, ii**. As mentioned above, all research about PMPC have reported the excellent biocompatible property suitable for biomedical application.

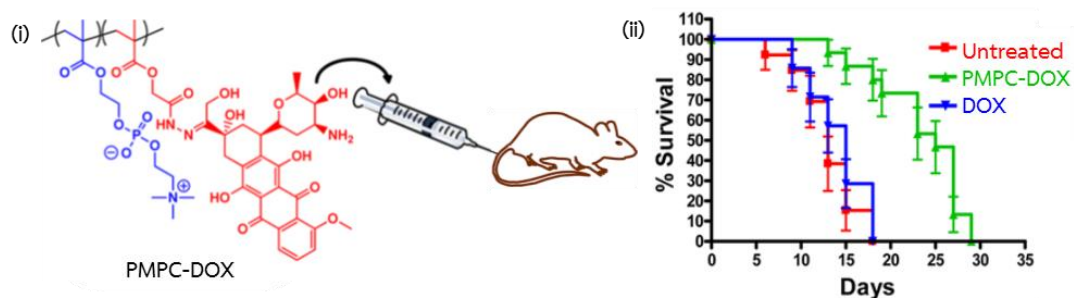


**Figure 1.7** (i) Structure of PMPC-DOX and (ii) survival curve for mice treated with PMAMPC-DOX [19].

Our group have recently introduced a novel platform for biosensing applications based on thiol-terminated poly[(methacrylic acid)-ran-(2-methacryloyloxyethyl phosphorylcholine)] (PMAMPC-SH) which was synthesized by reversible addition-fragmentation chain transfer (RAFT) polymerization. RAFT polymerization, one kind of controlled radical polymerization, has been successfully used for synthesizing the end-functionalized polymer in the presence of a reversible chain transfer reagent (CTA). By controlling the concentration of initiator and CTA, it is possible to produce polymer with controlled molecular weight and low polydispersity index (PDI) [20]. General mechanism for RAFT polymerization is shown in **Figure 1.8**. Upon aminolysis, the synthesized thiocarbonylthio end-PMAMPC would be converted to thiol-terminated PMAMPC that are available for grafting onto surfaces of gold [17]. The carboxyl groups from the MA units were attached with biotin. The presence of hydrophilic MPC units in the copolymer was found to be essential for suppressing unwanted non-specific adsorption and helped improving detection limit of target analyte, avidin in diluted blood plasma as monitored by SPR analysis. In light of this success, it is anticipated that this copolymer should be applicable for other biomedical applications. PMA units of the copolymer provide carboxyl groups as active sites for conjugation with desired biomolecule or drug whereas PMPC units should make materials to be interfaced with water soluble, biocompatible and anti-fouling.

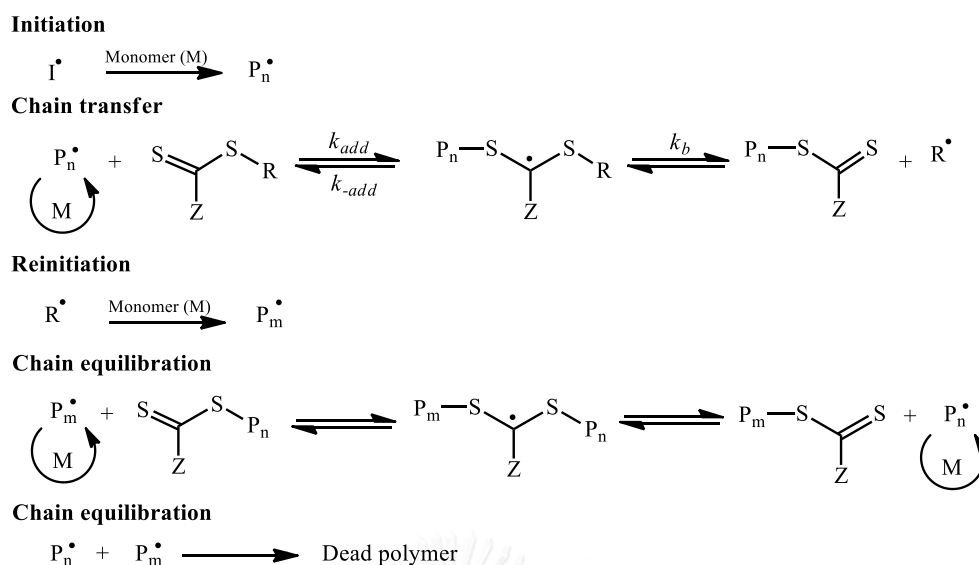


**Figure 1.8** The mechanism of RAFT polymerization[20].

Therefore, this research aims to develop anticancer drug delivery system based on AuNRs stabilized with PMAMPC. PMAMPC was first synthesized by reversible addition-fragmentation chain transfer (RAFT) polymerization and then conjugated with DOX by acid-labile hydrazone linkage. DOX-conjugated PMAMPC was then coated on AuNRs surface via ligand exchange with CTAB-stabilized AuNRs in order to get PMAMPC-DOX-AuNRs. Investigation on *in vitro* drug release and photothermal effect of the developed AuNRs was then performed. *In vitro* cytotoxicity and synergistic treatment against mammary gland adenocarcinoma (MDA-MB-231) cells were demonstrated by MTS assay. Intracellular DOX release was then verified using confocal laser scanning microscopy. Overall concept of this research work is summarized in **Figure 1.9**.

For a combination of photothermal process with chemotherapy providing synergistic effect on cancer cell damaging, thus enhancing efficiency of cancer therapy to achieve a pH-responsive drug release under acidic environment in lysosomes as shown in **Figure 1.9**.



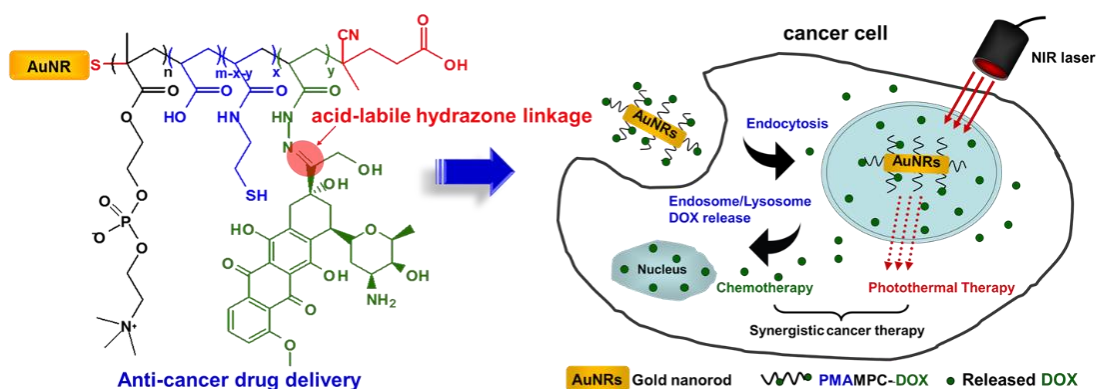


**Figure 1.9** Schematic illustration of AuNRs stabilized with DOX-conjugated PMAMPC (PMAMPC-DOX-AuNRs) for synergistic cancer therapy.

## 1.2 Objectives

- 1) To synthesize and characterize the AuNRs stabilized with drug-conjugated polymer.
- 2) *In vitro* studies of cytotoxicity, drug release, cellular uptakes and efficacy of chemo-, photothermal therapy of the developed AuNRs.

## 1.3 Scope of investigation

The stepwise investigation was carried out as follows:

- 1) Literature survey for related research work.
- 2) Synthesis and characterization of PMAMPC via RAFT polymerization.
- 3) Post polymerization modification of carboxyl groups in MA units of the copolymer.
- 4) Conjugation of DOX to modified PMAMPC by acid-labile hydrazone linkage.
- 5) *In vitro* drug release study of drug-conjugated polymer in buffer pH 5.0 and pH 7.4.
- 6) *In vitro* photothermal study of the developed AuNRs by NIR irradiation at 808 nm.
- 7) *In vitro* cytotoxicity test of the developed AuNRs against cancer cells, mammary gland adenocarcinoma (MDA-MB-231) cells by MTS assay.

8) Cellular uptake study of the developed AuNRs using confocal laser scanning microscopy.

9) *In vitro* synergistic therapy of the developed AuNRs by NIR irradiation at 808 nm.



## CHAPTER II

### MATERIALS AND METHODS

#### 2.1 Materials

2-Methacryloyloxyethyl phosphorylcholine (MPC) was purchased from NOF Corp. (Japan). Methacrylic acid (MA) was distilled under reduced pressure with added *p*-methoxyphenol (59 °C/13.5 mmHg). Doxorubicin hydrochloride (DOX.HCl) was purchased from CHEMIELIVA PHARMACEUTICAL CO., LTD. (Chongqing, China). 4,4'-azobis(4-cyanovaleric acid) (ACVA), 4-cyanopentanoic acid dithiobenzoate (CPD), hydrogen tetrachloroaurate (HAuCl<sub>4</sub>·3H<sub>2</sub>O), cetyltrimethylammonium bromide (CTAB, 97%), *L*-ascorbic acid, hydrazine monohydrate, phosphate buffered saline pH 7.4 (PBS) and dialysis bag (cutoff molecular weight of 3500 g/mol) were purchased from Sigma-Aldrich (USA). Silver nitrate (AgNO<sub>3</sub>), sodium borohydride (NaBH<sub>4</sub>) and ethanol were purchased from Merck (Germany). 1-(3-(Dimethylamino)propyl)-3-ethylcarbodiimide hydrochloride (EDC), *N*-hydroxysuccinimide (NHS) and cysteamine hydrochloride were purchased from Fluka (USA). 3-(4,5-Dimethylthiazol-2-yl)-5-(3-carboxymethoxyphenyl)-2-(4-sulfophenyl)-2H-tetrazolium (MTS) assay reagent containing the electron coupling agent phenazine ethosulfate (PES) was purchased from Promega (USA).

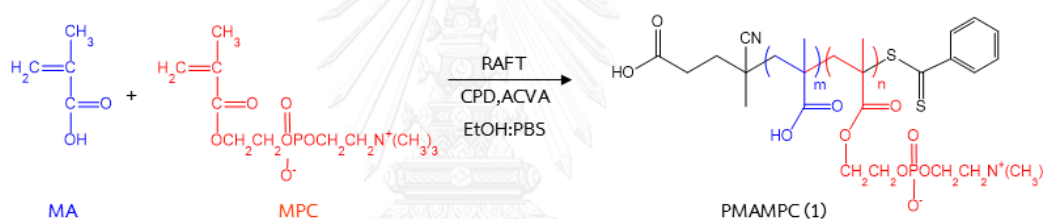
#### 2.2 Characterization

PMAMPC both before and after stepwise modification were characterized by nuclear magnetic resonance spectroscopy (NMR) in D<sub>2</sub>O using a Varian, model Mercury-400 nuclear magnetic resonance spectrometer (USA) operating at 400 MHz and Fourier transform infrared spectroscopy (FT-IR) using a Nicolet Impact 6700 FT-IR spectrometer with 32 scans at a resolution of 4 cm<sup>-1</sup> in a frequency range of 400-4000 cm<sup>-1</sup>. Samples were pressed into potassium bromide (KBr) pellets. UV-Vis spectra were recorded on an Agilent 8453 UV-Vis spectrometer in a quartz cell with 1 cm path length. The

morphology and size of AuNRs were analyzed by transmission electron microscopy (TEM) by a JEOL JEM-2010 (Japan) operating at 100 keV. The TEM samples were prepared by dropping approximately 10  $\mu\text{L}$  of the concentrated AuNRs on the carbon-coated copper grid which was dried in a desiccator before analysis. The average diameters of the observed AuNRs were reported from measurements of 50 random particles for each sample using SemAfore software. The Au element concentration in digested AuNRs sample was determined by inductively coupled plasma mass spectrometry (ICP-OES) by iCAP 6500 ICP-OES (Thermo Scientific, SciSpec CO., Ltd.).

## 2.3 Preparation of PMAMPC-DOX-AuNRs

### 2.3.1) Synthesis of PMAMPC by RAFT polymerization



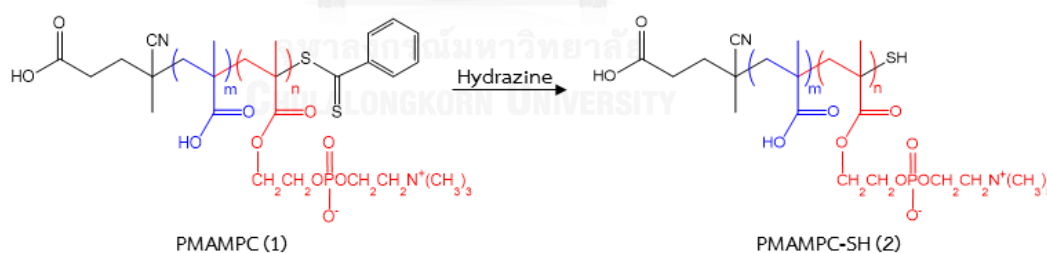
PMAMPC (1) having a targeted degree of polymerization (DP) of 100 and the comonomer composition (MA:MPC) of 80:20, 60:40, 40:60 was synthesized by RAFT polymerization. MPC monomer was dissolved in 1.87 mL of mixed solvent (1:1, EtOH: 1.0 M PBS in Milli-Q water). After the MPC monomer was completely dissolved, MA monomer, ACVA (2.6 mg, 9.35  $\mu\text{mol}$ ), and CPD (10.5 mg, 37.41  $\mu\text{mol}$ ) were added to the solution. To obtain copolymers with designated composition, the amount of MPC and MA were varied according to the ratios in **Table 2.1**. RAFT polymerization was operated under closed system under nitrogen atmosphere by capping the reaction bottle with septum and the solution was bubbled with  $\text{N}_2$  gas for 30 min and then put in an oil bath at 70  $^\circ\text{C}$  for 6 h. The polymer solution was purified by dialysis in DI water for 4 days and filtration by Whatman<sup>®</sup> qualitative filter paper, Grade 1 and then lyophilization, yielding orange cotton-like material with 65, 61 and 93% yield for PMAMPC having comonomer composition (MA:MPC)

of 80:20, 60:40 and 40:60, respectively. The composition of the copolymer was determined using  $^1\text{H}$  NMR spectroscopy.  $^1\text{H}$  NMR ( $\text{D}_2\text{O}$ , 400 MHz):  $\delta$  = 0.9 (s, 6H), 1.8 (br, 4H), 3.0 (s, 9H), 3.5 (s, 2H), 3.8-4.3 (m, 6H), 7.4-8.2 (m, 5H).

**Table 2.1** Varied amount of MA and MPC monomer for RAFT polymerization varied MA:MPC component

MA:MPC ratio	MA monomer		MPC monomer	
	Mol	Volume ( $\mu\text{L}$ )	Mol	Weight (g)
80:20	$2.99 \times 10^{-3}$	233.8	$7.48 \times 10^{-4}$	0.2012
60:40	$2.24 \times 10^{-3}$	190.3	$1.50 \times 10^{-3}$	0.4425
40:60	$1.50 \times 10^{-3}$	126.9	$2.24 \times 10^{-3}$	0.6637

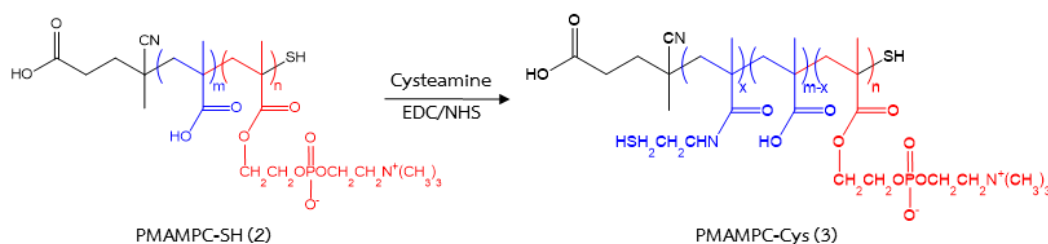
### 2.3.2) Synthesis of Thiol-terminated PMAMPC (PMAMPC-SH)



Hydrazine (10-30 mole equiv to dithiobenzoate group) was added to the 5 mM PMAMPC solution in Milli-Q water and then stirred at ambient temperature for 1 h or until the polymer solution became colorless. When the addition was complete, the solution was added dropwise to 1.0 M HCl (aq) (10 mL). The obtained PMAMPC-SH (2) was purified by dialysis in HCl solution pH 3.0 and DI water for 2 days each. The white cotton-like product of PMAMPC-SH was obtained after lyophilization. PMAMPC (1) and PMAMPC-SH (2) were characterized using  $^1\text{H}$

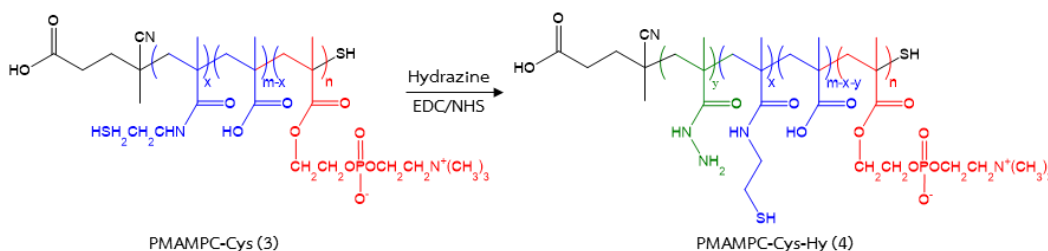
NMR, UV-vis and FT-IR spectroscopies.  $^1\text{H}$  NMR ( $\text{D}_2\text{O}$ , 400 MHz):  $\delta$  = 0.9 (s, 6H), 1.8 (br, 4H), 3.0 (s, 9H), 3.5 (s, 2H) and 3.8-4.3 (m, 6H).

### 2.3.3) Modification of PMAMPC-SH with Cysteamine



PMAMPC-SH (2) having 50:50 MA:MPC composition (120 mg, 0.313 mmol of MA unit) was dissolved in 2 mL of Milli-Q water. To activate carboxyl groups, EDC (0.2 M) and NHS (0.1 M) were added to PMAMPC-SH solution and stirred for 30 min. After that, cysteamine (0.1 mol equiv to MA unit) was added and stirred overnight. The product was purified by dialysis in DI water for 3 days. After lyophilization, white solid of PMAMPC-Cys (3) was obtained and characterized by FT-IR spectroscopy.

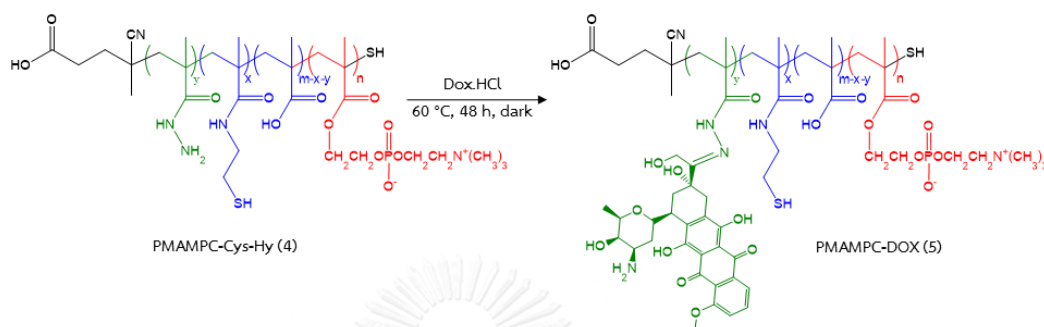
### 2.3.4) Modification of PMAMPC-Cys with Hydrazine



PMAMPC-Cys (3) (95 mg, 0.247 mmol of MA unit) was dissolved in 1.2 mL of Milli-Q water. To activate the remaining carboxyl groups in the copolymer, EDC (0.2 M) and NHS (0.1 M) were added to PMAMPC-Cys (3) solution and stirred for 30 min. After that, hydrazine (20 mol equiv to MA unit) was added and stirred overnight. The product was purified by dialysis in DI water for 3 days. After

lyophilization, white cotton-like product of PMAMPC-Cys-Hy (4) was characterized by FT-IR spectroscopy.

### 2.3.5) Conjugation of Doxorubicin



The mixture of PMAMPC-Cys-Hy (4) (0.01 mmol, 4.0 mg) and DOX.HCl (1:1 mol ratio of DOX:COOH group in PMAMPC (1)) in 5 mL of Milli-Q water was stirred in the dark at 60°C for 2 days. The resulting conjugate was purified by dialysis in Milli-Q water for 4 days. PMAMPC-DOX (5) was obtained as dark red cotton-like product after lyophilization then characterization by FT-IR spectroscopy. The DOX loading of the conjugate was calculated on the basis of UV-Vis absorbance at 485 nm, using the calibration curve of DOX at 485 nm.

### 2.3.6) Synthesis of AuNRs by Seed-mediated Growth method

All glasswares were clean and rinsed with aqua regia (HCl:HNO<sub>3</sub> = 3:1 by volume) prior to use. Solutions of ascorbic acid, AgNO<sub>3</sub>, HAuCl<sub>4</sub>, and NaBH<sub>4</sub> were freshly prepared in Milli-Q water. This reaction was carried out at room temperature (≈27°C). Colloidal gold seed nanospheres (having a diameter of ~1.5–4.0 nm) were first prepared by rapidly injecting 0.50 mL of ice-cold 10.0 mM NaBH<sub>4</sub> solution into a vigorously stirred aqueous solution containing HAuCl<sub>4</sub> (1.44 M, 1.25 μL in 1.12 mL of Milli-Q water) and CTAB (0.20 M, 2.50 mL). The solution was continuously stirred for 2 min. Afterwards, the reaction was allowed to proceed for 1 h to form the CTAB-capped Au nanoparticles to be used as seeds for the synthesis of AuNRs.

To synthesize the AuNRs, ascorbic acid ( $7.88 \times 10^{-2}$  M, 62.00  $\mu\text{L}$ ) was added gently into the growth solution containing  $\text{HAuCl}_4$  (1.44 M, 2.60  $\mu\text{L}$  in Milli-Q 2.25 mL),  $\text{AgNO}_3$  (4.00 mM, 140  $\mu\text{L}$ ), and CTAB (0.20 M, 2.50 mL). After the orange-colored solution became colorless, 50.00  $\mu\text{L}$  of the seed solution was rapidly mixed. The solution color changed to brown-red.

The solution of CTAB-AuNRs (4.00 mL) was washed for 2 centrifugation-resuspension cycles (14 krpm for 15 min). After that, concentrated AuNRs was digested in 0.50 mL of aqua regia for 30 min. The volume of solution was adjusted to 5.00 mL and filtered using 0.45  $\mu\text{m}$  syringe. The Au element concentration was determined by iCAP 6500 ICP-OES (Thermo Scientific, SciSpec CO., Ltd.) using the calibration curve of  $\text{HAuCl}_4$ .

### 2.3.7) Preparation of Polymer-stabilized AuNRs via Ligand Exchange

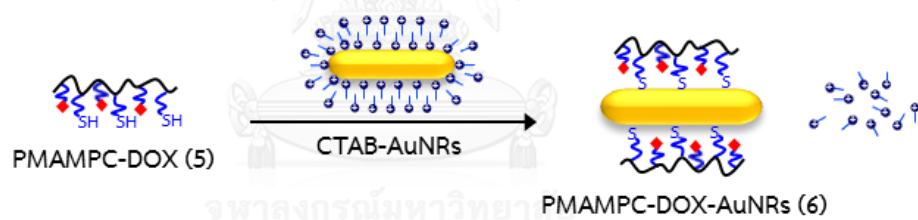


**Figure 2.1** Schematic illustration of ligand exchange process.

CTAB-AuNRs solution (0.50 mL) was purified by two centrifugation-resuspension cycles (14 krpm, 10 min). Each centrifugation cycle was followed by dispersion in Milli-Q water to attain the same final volume. The CTAB-AuNRs solution was added dropwise to aqueous solution of PMAMPC-SH (2) (3.1 mg in 1 mL of 10 mM PBS). The mixture was sonicated for 15 min and incubated for 2 days at ambient temperature. To remove the unbound ligand, the mixture was centrifugally washed for three times (14 krpm, 10 min) and re-dispersed in 0.5 mL of 10 mM PBS. The purified AuNRs before and after ligand exchange were characterized by UV-Vis spectroscopy and TEM. For the AuNRs stabilized by



PMAMPC-Cys (3) or PMAMPC-DOX (5), they were prepared following the same procedure.

### **2.3.8) Determination of the DOX loading content on AuNRs by Cyanide Digestion**

The DOX loading content (DLC), defined as the weight percent of DOX in the AuNRs nanocarriers, was quantified by UV-Vis analysis. First, PMAMPC-DOX-AuNRs (6) were washed by 2 centrifugation-redispersion cycles (14 krpm, 10 min/cycle) to remove unbound PMAMPC-DOX (5). After that, 1 mL of 12 mM KCN solution was added to the concentrated PMAMPC-DOX-AuNRs and incubated at ambient temperature for 2 days. The absorbance of DOX at 485 nm was measured to determine the DLC in the solution using a previously established calibration curve. The DLC measurements were performed in triplicate for each sample. The absorption of digested PMAMPC-Cys-AuNRs was defined as blank.

## **2.4 *In vitro* Drug Release Studies**

The pH-responsive DOX release from PMAMPC-DOX (5) was performed in acetate buffer (10 mM, pH 5.0) and phosphate buffer (10 mM, pH 7.4) using a dialysis method. An aliquot (1.0 mL) of PMAMPC-DOX (4.0 mg) was loaded in a dialysis bag and immediately placed in 20 mL of corresponding buffer at ambient temperature under stirring. Periodically, 1 mL of the buffer solution outside the dialysis bag was taken out and replaced with equal volume of fresh medium. The amount of DOX was quantified by measuring its absorbance at 485 nm against a standard curve.

## **2.5 *In vitro* Photothermal Studies**

The potential application of AuNRs for photothermal therapy was investigated by measuring the temperature rise of PMAMPC-DOX-AuNRs (6) solution upon irradiation by NIR laser. 2.0 mL of PMAMPC-DOX-AuNRs aqueous suspensions at various AuNRs

concentrations (0, 2, 4, 6, 8 and 10  $\mu\text{g}/\text{mL}$ ) was prepared in a glass tube and irradiated with a NIR laser (2W 800 nm Diode Laser; MDL-III-800-2000, Ultralasers, Inc., Canada) for 15 min. Temperature was detected by the ETI MicroTherma 2T thermometer at a time interval of 1 min.

## 2.6 Cell culture

Mammary gland adenocarcinoma (MDA-MB-231) cells were cultured in Minimum Essential Medium with Earle's Balanced Salts (MEM/EBSS, GE Healthcare HyClone) containing 1 % of MEM Non-Essential Amino Acids (NEAA, GE Healthcare HyClone), 10% of fetal bovine serum (FBS, GIBCO) and 1 % of penicillin-streptomycin (pen-step, GE Healthcare HyClone) at 37 °C under 5% CO<sub>2</sub> condition. Cells were cultured for 2 days to achieve approximately same confluency before performing all experiments.

## 2.7 *In vitro* Cytotoxicity Assay

Cytotoxicity of all modified AuNRs was examined using a colorimetric MTS cell viability assay. A 100  $\mu\text{L}$  suspension of MDA-MB-231 cells ( $5,000 \text{ cells}\cdot\text{mL}^{-1}$ ) was plated onto 96-well plates, cultured for 24 h, then replaced with 100  $\mu\text{L}$  of various concentrations of PMAMPC-DOX-AuNRs, PMAMPC-Cys-AuNRs and DOX in MEM and maintained at 37 °C under 5% CO<sub>2</sub> condition for 24 h. 100  $\mu\text{L}$  of the same concentrations of PMAMPC-DOX-AuNRs, PMAMPC-Cys-AuNRs and DOX in MEM was defined as a blank. 10  $\mu\text{L}$  of MTS solution was added. After 4 h, the absorbance at 492 nm of the resulting cell suspension was determined by a microplate reader (Biochrom<sup>®</sup> Anthos 2010, UK) and data were analyzed using ADAP 2.0 Basic software. The absorbance of treated cell suspensions were subtracted with their blank and compared to the untreated wells to deduce cell viability.

## 2.8 Cellular Uptake Study

MDA-MB-231 cells ( $2.5 \times 10^5$  cells) were seeded into an 8-well Lab-Tek II Chamber Slide w/Cover RS Glass Slide in 500  $\mu\text{L}$  of MEM, and cultured for 24 h. The media was removed and a total of 500  $\mu\text{L}$  of free DOX, PMAMPC-DOX or PMAMPC-DOX-AuNRs solution (15  $\mu\text{g}$  DOX/mL) was added immediately. After incubation with sample solutions for 30 and 120 min, cells were gently washed with 500  $\mu\text{L}$  of PBS twice, followed by an addition of 100  $\mu\text{L}$  of DAPI (0.02 mg/mL), nucleus staining dye, and then incubated at ambient temperature in dark for 5 min with shaking. After staining, cells were gently washed with 500  $\mu\text{L}$  of PBS three times. Chamber was removed from glass slide. The glass slide was allowed to dry then dropped with MOWIOL, anti-phade reagent, after that closed with cover slip. Confocal laser scanning microscopic (CLSM) analysis of these cells was performed on FluoView FV10i confocal microscope (OLYMPUS) and the images were analyzed using FV10-ASW 4.2 Viewer software.

## 2.9 *In vitro* Synergistic Therapy

The efficacy of PMAMPC-DOX-AuNRs (6) in synergistic therapy was examined using a colorimetric MTS cell viability assay. A 100  $\mu\text{L}$  suspension of MDA-MB-231 cells (5,000 cells/mL) was seeded onto 96-well plates and cultured for 24 h. After that, media was replaced with 100  $\mu\text{L}$  of PMAMPC-DOX-AuNRs, PMAMPC-Cys-AuNRs and DOX (AuNRs concentration: 5  $\mu\text{g}$ /mL). 100  $\mu\text{L}$  of PMAMPC-DOX-AuNRs, PMAMPC-Cys-AuNRs and DOX at the same concentration in MEM was used as a blank. After incubated with sample solutions for 24 h at 37 °C under 5% CO<sub>2</sub> condition for 24 h, Suspensions in selected wells were then irradiated with NIR laser (2W 800 nm Diode Laser; MDL-III-800-2000, Ultralasers, Inc., Canada) from the top with distance  $\sim$  15 cm for 30, 45 and 60 sec. Cells without irradiation were used as a control. After irradiation treatment, cells were cultured for another 24 h. Then, the cell viability was determined by MTS

assay by adding 10 mL of MTS solution into each well. After 4 h, the absorbance at 492 nm was measured on a microplate reader to check the cells' survival.



## CHAPTER III

### RESULTS AND DISCUSSION

#### 3.1 Preparation and Characterization of PMAMPC-DOX-AuNRs

##### 3.1.1) Preparation of PMAMPC and Thiol-Terminated PMAMPC (PMAMPC-SH)

PMAMPC was synthesized using RAFT polymerization in the presence of CPD and ACVA as chain transfer agent (CTA) and radical initiator, respectively. The ratio of CTA/initiator or  $[CTA]/[I]$  was fixed at 4/1[17]. From  $^1\text{H-NMR}$  spectra of PMAMPC shown in **Figure 3.1**, characteristic peaks of the MPC unit ( $-\text{N}(\text{CH}_3)_3 = 3.0$  ppm,  $-\text{CH}_2\text{N}$  (d) = 3.5 ppm, and  $-\text{POCH}_2\text{CH}_2\text{N} - \text{COOCH}_2 - \text{CH}_2\text{CH}_2\text{OP} = 3.8\text{-}4.3$  ppm) were clearly observed. The copolymer composition (MA:MPC) determined from  $^1\text{H-NMR}$  spectra (**Figure 3.1**, i) by integrating peak b,b' at  $\delta$  0.9 ppm ( $\text{CH}_3$  proton of both MPC and MA) and peak d at  $\delta$  3.5 ppm ( $\text{CH}_2$  protons of MPC) against peak f at around 7.4-8.2 ppm (protons of aromatic). The results displayed in **Table 3.1** suggested that the targeted DP and molecular weight ( $M_n$ ) of PMAMPC can be reached. The copolymer composition determined by  $^1\text{H NMR}$  closely resembled the comonomer ratio in the feed for the copolymers with targeted MA:MPC of 80:20 and 60:40, suggesting that the copolymer with varied composition can be synthesized. Except for the copolymer with targeted MA:MPC of 40:60, its calculated MPC composition reached as high as 82%. This may be explained as a result of greater polymerization kinetic of MPC as compared with MA so that its incorporation into the copolymer becomes superior especially when its feed composition is greater than MA.

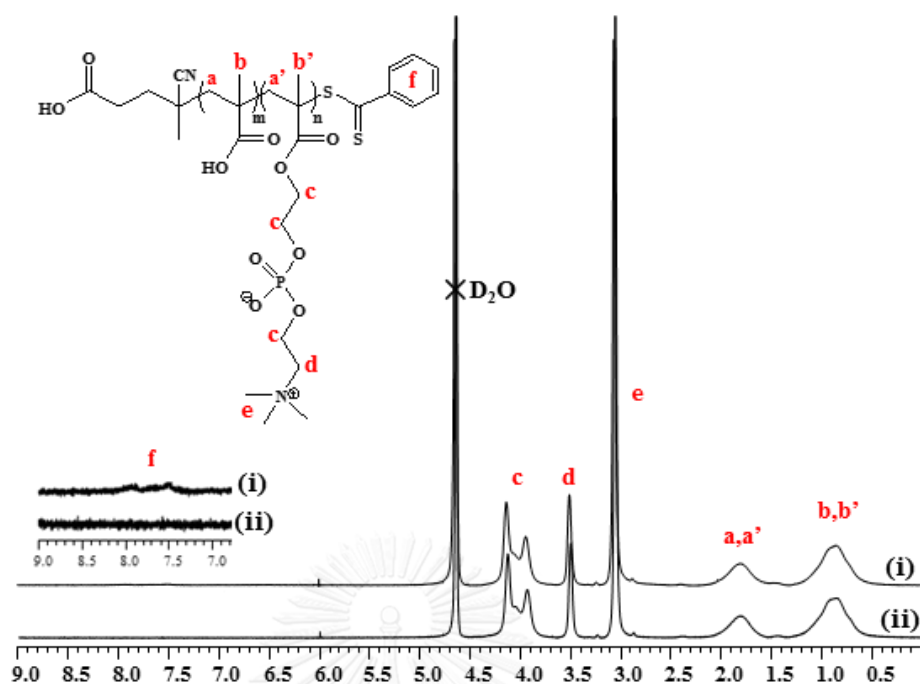


**Figure 3.1**  $^1\text{H}$  NMR spectra of PMAMPC (i) and PMAMPC-SH (ii) in  $\text{D}_2\text{O}$ .

**Table 3.1** Summary of composition and molecular weight of PMAMPC copolymer

DP	In feed			In copolymer			
	%MA	%MPC	$M_n$ (Da)	DP <sub>a</sub>	%MA <sup>a</sup>	%MPC <sup>a</sup>	$M_n$ (Da) <sup>a</sup>
100	80	20	13,078	124	78	22	16,611
100	60	40	17,270	110	50	50	21,275
100	40	60	21,462	167	18	82	43,369

<sup>a</sup> Determined by  $^1\text{H}$ -NMR in  $\text{D}_2\text{O}$

The dithiobenzoate group at the chain end of PMAMPC was converted to a thiol group by reduction using hydrazine. The disappearance of peak assigned to aromatic protons around  $\delta$  7.4–8.2 ppm in  $^1\text{H}$  NMR spectrum (**Figure 3.1**, ii) after reduction indicated that the dithiobenzoate group at the chain end of PMAMPC was successfully eliminated yielding PMAMPC-SH having a thiol end. The success of reduction was also confirmed from the vanishing of UV absorbance at 306 nm (**Figure 3.2**).

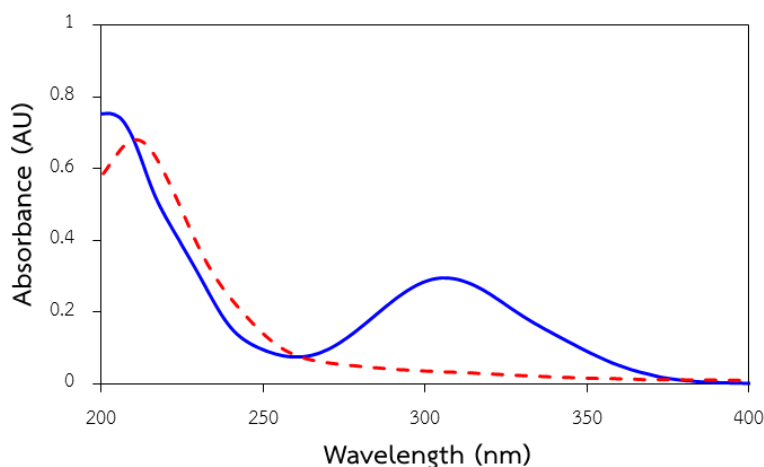
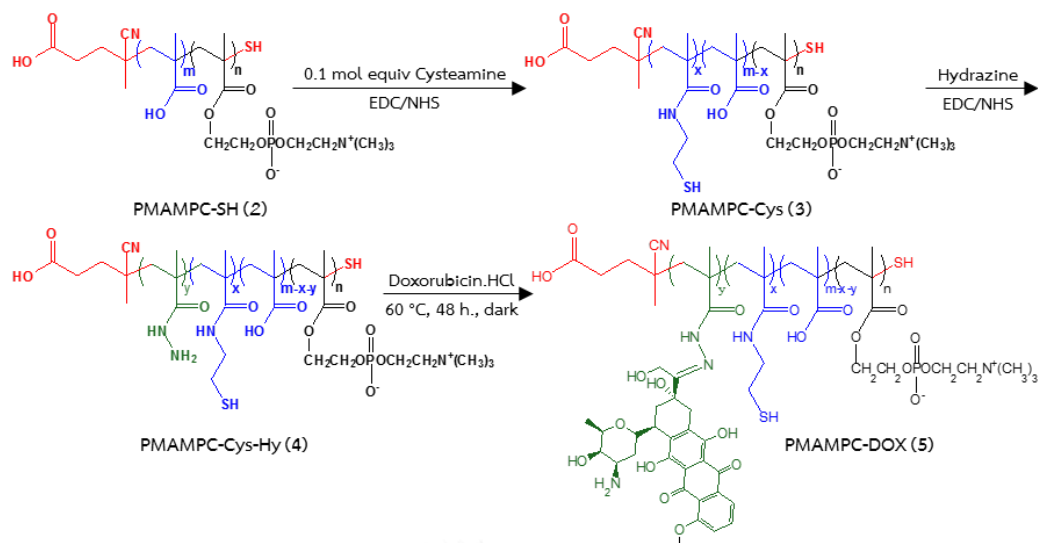


**Figure 3.2** UV-vis absorption spectra of PMAMPC DP100 (MA:MPC = 50:50) before (—) and after (---) reduction.

### 3.1.2) Modification of PMAMPC-SH and Doxorubicin Conjugation

Previously, we have attempted to prepare AuNRs stabilized by PMAMPC-SH via ligand exchange of the CTAB-stabilized AuNRs with PMAMPC-SH. It was found that the resulting AuNRs were not stable and aggregated in spite of copolymer composition implying that the number of active thiol binding sites only available at the chain ends of PMAMPC-SH are not enough to yield stable AuNRs. For this reason, we have desired to add more thiol groups to the PMAMPC-SH prior to modification with hydrazine and DOX conjugation. PMAMPC having MA:MPC of 50:50 was chosen for this investigation mainly because the AuNRs stabilized by the PMAMPC-SH at this composition possessed the least degree of aggregation.

As outlined in **Scheme 3.1**, to introduce more thiol groups for Au-S formation, some carboxyl groups of PMAMPC-SH was modified with cysteamine via amide linkage using EDC/NHS as coupling agent yielding PMAMPC-Cys. The remaining carboxyl groups were then covalently bonded with excess hydrazine to give PMAMPC-Cys-Hy that was further conjugated with DOX. The success of stepwise modification of PMAMPC-SH and subsequent DOX conjugation was verified by FT-IR analysis of which data are displayed in **Figure 3.3**.



**Scheme 3.1** Synthetic route employed for the preparation of PMAMPC-DOX.

From FTIR spectrum of PMAMPC-SH (**Figure 3.3**, i), characteristic peaks of MPC unit appear at 798, 970, 1085, 1176, and 1230  $\text{cm}^{-1}$ , assignable to C-O-P,  $\text{N}^+(\text{CH}_3)_3$ , P-O, C-O, and P=O, respectively. C=O Stretching of carboxyl group in MA unit appears at 1720  $\text{cm}^{-1}$ . Relative intensity between the peak at 1631  $\text{cm}^{-1}$  which is contributed to amide C=O/C=N stretching and the peak at 1720  $\text{cm}^{-1}$  corresponding to C=O stretching of COOH groups proportionally increased after modification. The former peak dominated the latter one after DOX conjugation. This evidently verified the success of stepwise chemical modification. Additional amide bonds were formed between the carboxyl groups of PMAMPC-SH and cysteamine and hydrazine. Besides, the N-H bending of PMAMPC-Cys-Hy was also found at 1560  $\text{cm}^{-1}$ .



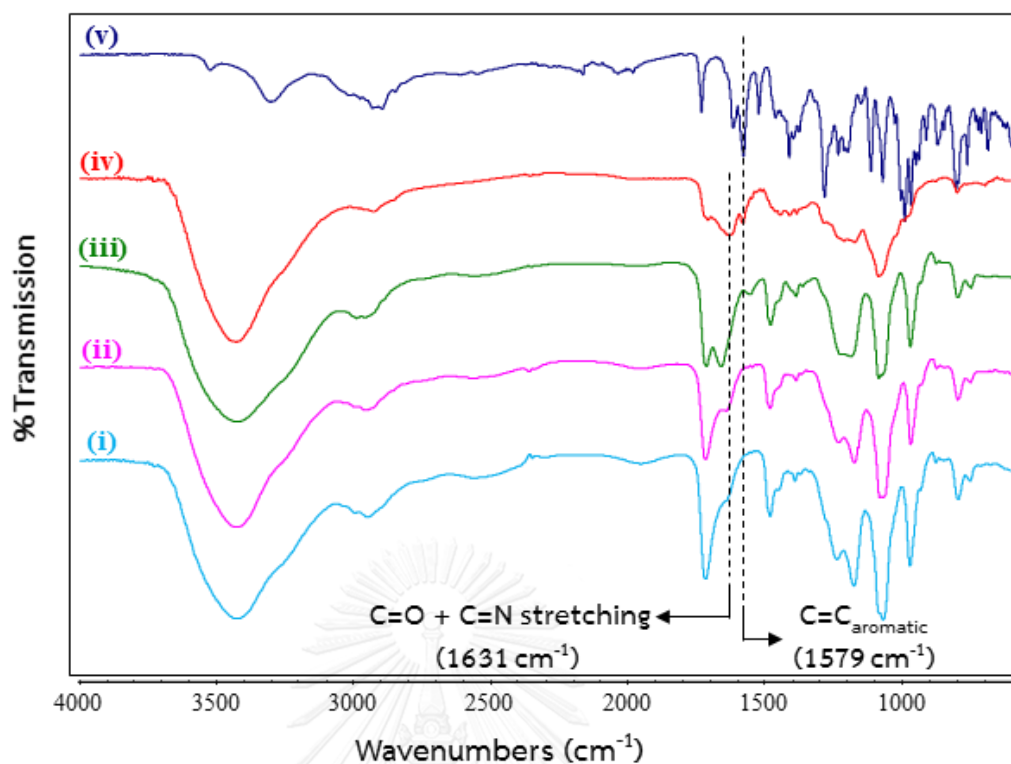


**Figure 3.3** FTIR spectra of (i) PMAMPC-SH, (ii) PMAMPC-Cys, (iii) PMAMPC-Cys-Hy, (iv) PMAMPC-DOX, and (v) DOX.

In **Figure 3.4**, PMAMPC-DOX exhibited the absorption of DOX with  $\lambda_{\max} \sim 485$  nm that also confirms the conjugation of DOX. Moreover, DOX loading of the conjugate was calculated on the basis of UV-Vis absorbance at 485 nm, using the calibration curve of DOX. PMAMPC-DOX contained DOX loading about 34.3 %wt. This DOX loading is relative high in comparison to previously reported work also based on DOX-conjugated polymer (typically  $\sim 10$ – $20$  wt %) [14].

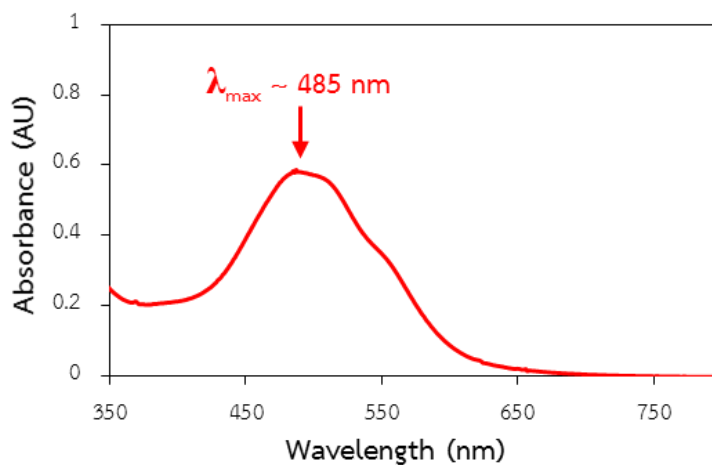
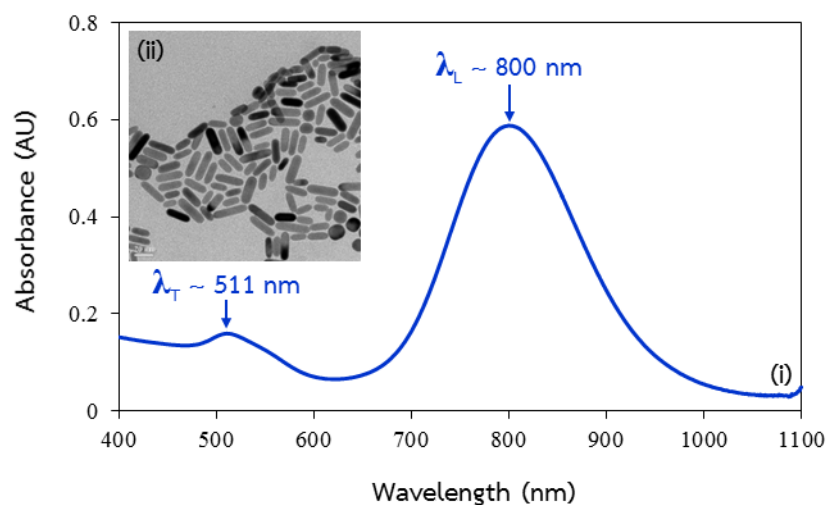


**Figure 3.4** UV-Vis absorption spectra of PMAMPC-DOX in Milli-Q water.

### 3.1.3) Synthesis of AuNRs by Seed-mediated Growth Method (CTAB-AuNRs)

From **Figure 3.5**, i, the SPR band of AuNRs typically splits into two, corresponding to a transverse (short axis) band ( $\lambda_T$ ) at 511 nm and a longitudinal (long axis) band ( $\lambda_L$ ) at 800 nm in NIR region, whose positions depend on aspect ratio (length/width) of AuNRs. As determined by TEM, CTAB-AuNRs (**Figure 3.5**, ii) were quite uniform in size with  $8.2 \pm 1$  nm in width and  $31.6 \pm 3$  nm in length with aspect ratio  $\sim 3.72$ . We found that few Au nanospheres mingled in the solution.

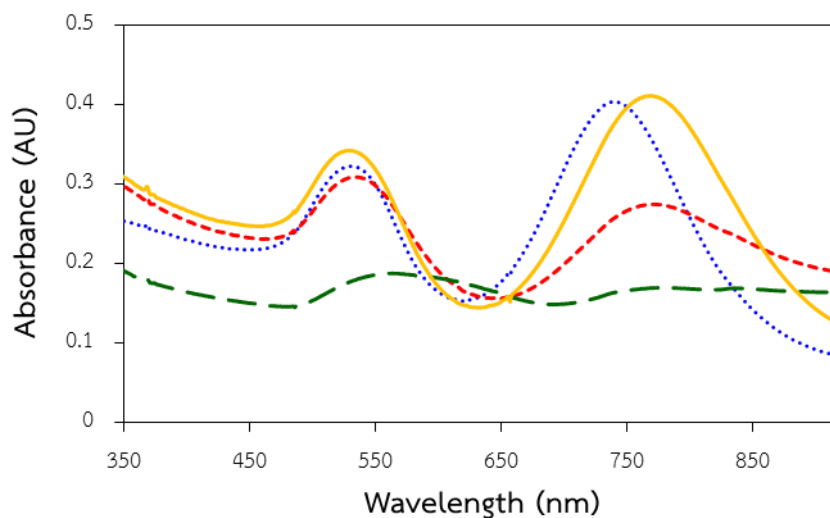
To determine a concentration Au element, CTAB-AuNRs were first washed in order to remove the  $\text{Au}^{3+}$  residue or very small AuNRs in supernatant. The concentrations of Au element were then determined using inductively coupled plasma optical emission spectrometry (ICP-OES). The synthesized CTAB-AuNRs consisted of Au element concentration about of  $\pm 0.4 \mu\text{g/mL}$  ( $n=3$ ).



**Figure 3.5** (i) UV-Vis absorption spectra of CTAB-AuNRs prepared by seed-mediated growth method and (ii) TEM image of CTAB-AuNRs (scale bar 20 nm).

#### 3.1.4) Preparation of Polymer-stabilized AuNRs via Ligand Exchange

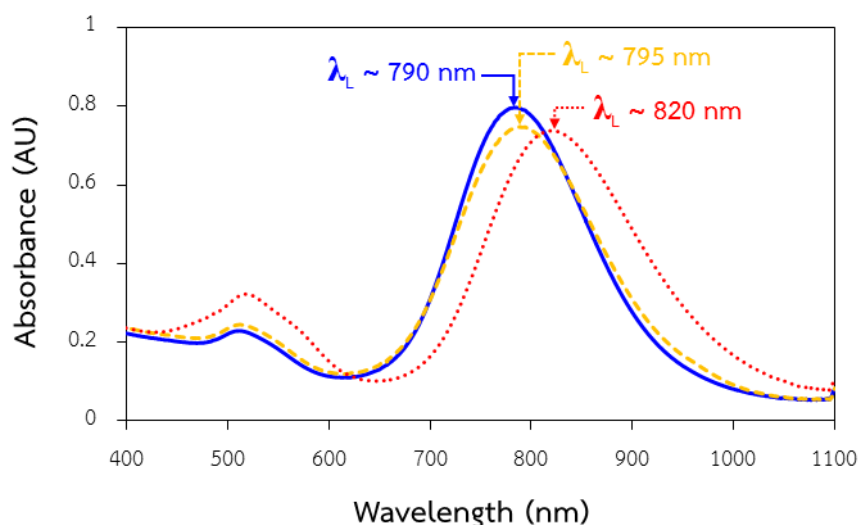
PMAMPC-SH was coated onto AuNRs surface through Au-S formation via ligand exchange process. The copolymers having varied MA:MPC composition were tested. Some aggregation of AuNRs occurred as can be visualized by naked eye. The color of AuNRs suspension was changed from brown-red to blue for all copolymers. Such change can also be realized from the red shift of the peak at the wavenumber 745 nm as analyzed by UV-Vis analysis (**Figure 3.6**). Precipitation of the PMAMPC-AuNRs was only observed for the copolymer with the composition of 78:22 (MA:MPC) of which MPC content was the lowest among the copolymers investigated. This may presumably be describable to the reduced solubility of the copolymer as the hydrophilic MPC composition decreased. Its UV-Vis spectrum almost disappeared indicating that the AuNRs were no longer dispersible in water.



**Figure 3.6** UV-Vis absorption spectra of PMAMPC- AuNRs suspension in 10 mM PBS having varied MA:MPC composition; 78:22 (— —), 50:50 (— —), 29:71 (— —), and CTAB-AuNRs (.....).

Due to the least aggregation of PMAMPC-AuNRs prepared from PMAMPC having MA:MPC of 50:50 was therefore chosen for further modification with cysteamine in order to increase the active binding sites for each PMAMPC chains before coating AuNRs surface to provide better colloidal stability.

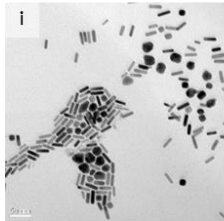
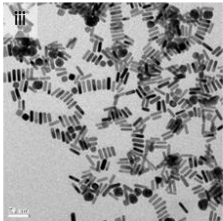
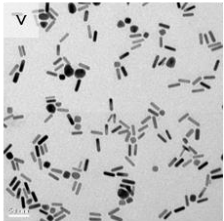
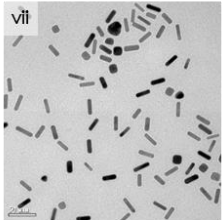
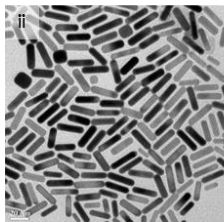
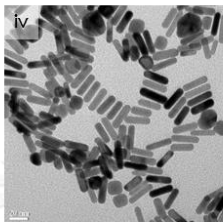
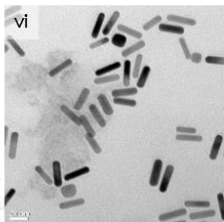
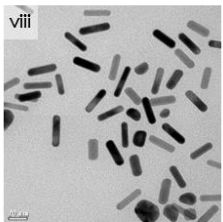
As shown in **Figure 3.7**, the  $\lambda_L$  of synthesized CTAB-AuNRs appeared at 790 nm. The fact that  $\lambda_L$  of PMAMPC-Cys-AuNRs was about 795 nm without broadening and tailing as compared with that of the CTAB-AuNRs suggested that additional thiol groups introduced from cysteamine to PMAMPC can provide greater active binding sites for anchoring to the AuNRs surface and thus yielded PMAMPC-Cys-AuNRs with good colloidal stability in 10 mM PBS. Likewise, upon ligand exchange, the obtained PMAMPC-DOX-AuNRs were quite stable as can be realized from their UV-Vis absorption (**Figure 3.7**) appearing at 820 nm, only slightly red-shifted from 790 nm of the as-synthesized CTAB-AuNRs. Neither broadening nor tailing of the SPR band of PMAMPC-DOX-AuNRs was observed that indicated no aggregation of the particle arisen during this step [13]. Broad absorption band around 485 nm can confirm the presence of PMAMPC-DOX on PMAMPC-DOX-AuNRs.



**Figure 3.7** UV-vis absorption spectra of CTAB-AuNRs (—), PMAMPC-Cys-AuNRs (---) and PMAMPC-DOX-AuNRs (···) suspension in 10 mM PBS.

Morphology of all AuNRs was characterized by TEM. PMAMPC-AuNRs (MA:MPC=50:50) showed some aggregation in TEM images (**Figure 3.2**, iii-iv). This is consistent with their absorption results previously shown in **Figure 3.2**. Coating the AuNRs with PMAMPC-Cys and PMAMPC-DOX provide steric stabilization and can apparently improve dispersibility of the AuNRs (**Table 3.2**, v-vi and vii-viii). PMAMPC-DOX-AuNRs were quite uniform in size with  $8.2 \pm 1$  nm in width and  $31.6 \pm 3$  nm in length and much more well-dispersed than the CTAB-AuNRs. The aspect ratio ( $\sim 3.7$ ) remained unchanged after ligand exchange suggesting that polymer coating does not affect the AuNRs morphology. Moreover, the results observed by TEM are in good agreement with the UV-Vis absorption data.

**Table 3.2** Morphology information of the developed AuNRs

Magnification	CTAB-AuNRs	PMAMPC-SH-AuNRs	PMAMPC-Cys-AuNRs	PMAMPC-DOX-AuNRs
50 nm				
20 nm				
Length (nm) <sup>a</sup>	26.7 ± 4	25.9 ± 3	26.8 ± 3	26.9 ± 3
Width (nm) <sup>a</sup>	7.6 ± 3	7.6 ± 1	7.3 ± 1	7.4 ± 1
Aspect ratio	3.5	3.4	3.7	3.7

<sup>a</sup> The average diameters of the observed AuNRs were reported from measurements of 50 random particles for each sample using SemAfore software.

### 3.1.5) Determination of the DOX Loading Content of AuNRs by Cyanide Digestion

CTAB-AuNRs are recognized to degrade completely within few minutes of exposure to 12 mM sodium cyanide solution. This degradation process becomes slower when AuNRs are coated with polymeric ligands [18]. In the cases of PMAMPC-Cys-AuNRs and PMAMPC-DOX-AuNRs, it was found that it took 48 h to completely digest the AuNRs suggesting that the functionalized AuNRs are sufficiently protected by the polymer coating. The progress of digestion was monitored by UV-Vis spectroscopy as shown in **Figure 3.8**. The disappearance of

SPR band at 820 nm of PMAMPC-DOX-AuNRs was observed indicating that AuNRs were completely digested.

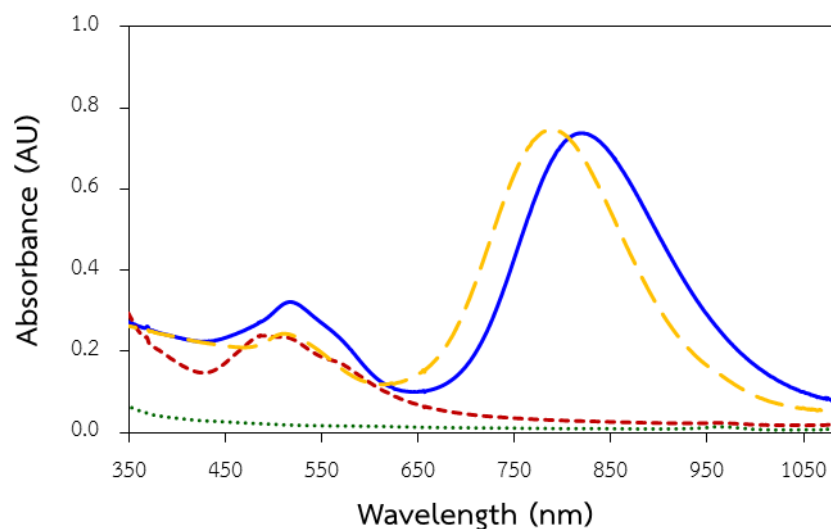


**Figure 3.8** UV-vis absorption spectra of PMAMPC-DOX-AuNRs before (—) and after (---) digestion and PMAMPC-Cys-AuNRs before (---) and after (.....) digestion.

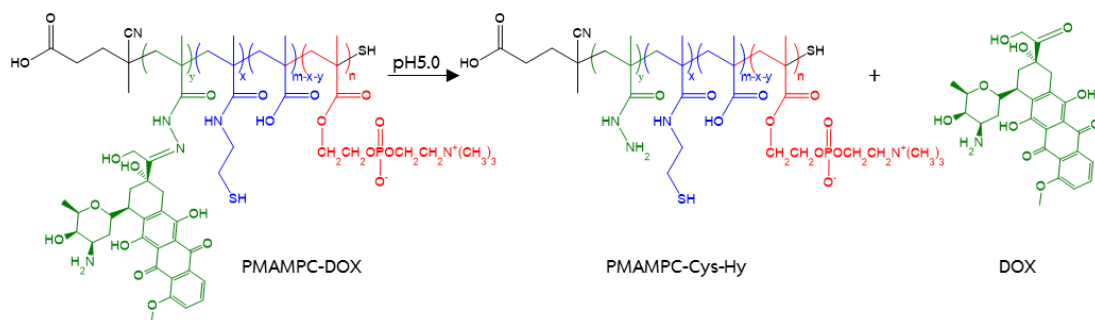
The DOX loading content (DLC), defined as the weight percent of DOX in the developed AuNRs, was quantified by UV-Vis analysis. After cyanide digestion, DOX in solution was calculated on the basis of UV-Vis absorbance at 485 nm, using the calibration curve of DOX at 485 nm. The absorption of digested PMAMPC-Cys-AuNRs was defined as blank. The DLC was found to be about 19 %wt.

### 3.2 *In vitro* Drug Release Studies

Conjugation of DOX to the PMAMPC-Cys-Hy by an acid-labile hydrazone bond initiated that PMAMPC-DOX should show lysosomal pH-triggered DOX release (**Scheme 3.2**). To demonstrate the pH-sensitive drug release behavior of PMAMPC-DOX, *in vitro* DOX release was measured as a function of time in pH 7.4 and 5.0 buffers.

As shown in **Figure 3.9**, DOX release can apparently be accelerated under acidic condition at pH 5.0, the value close to the acidic environment of lysosome compartments ( $\sim 4.5\text{--}5.0$ ) [14] with as high as 86% accumulated release after 48 h as

opposed to only 37% of DOX released after the same period of time upon incubation at pH 7.4. This set of data thereby demonstrates the efficacy of pH-sensitive drug release from PMAMPC-DOX at acidic environment like endo/lysosome.



**Scheme 3.2** pH-sensitive DOX release behavior of PMAMPC-DOX.

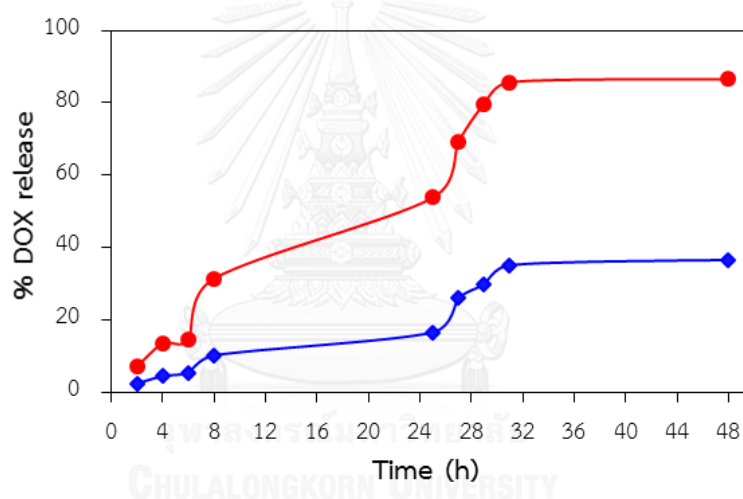


**Figure 3.9** *In vitro* drug release measurement of PMAMPC-DOX-AuNRs DOX release profile from PMAMPC-DOX in pH 5.0 (dot point) and pH 7.4 (square point) buffers.

### 3.3 *In vitro* Photothermal Studies

To determine the photothermal effect of AuNRs, aqueous suspensions of PMAMPC-DOX-AuNRs were exposed to NIR laser irradiation at 808 nm with power density 2 W/cm<sup>2</sup>. Changes in temperature were detected using a thermometer. As shown in **Figure 3.10**, both the temperature elevation rate and final temperature were dependent on quantity of Au element; a faster and greater temperature increase was



observed for a higher quantity of Au element. 2 mL of PMAMPC-DOX-AuNRs suspension having 20  $\mu\text{g}$  Au element can reach as high as 70.1°C (increased by 39.7 °C) after 15 min irradiation. The temperature of AuNRs-free solution (10 mM PBS) increased by only 4.4 °C under the same experimental conditions. It is notably that the continuous laser irradiation affected no loss of the optical properties of AuNRs and no change of particle size, indicating that PMAMPC-DOX-AuNRs were stable under laser irradiation and temperature increase.

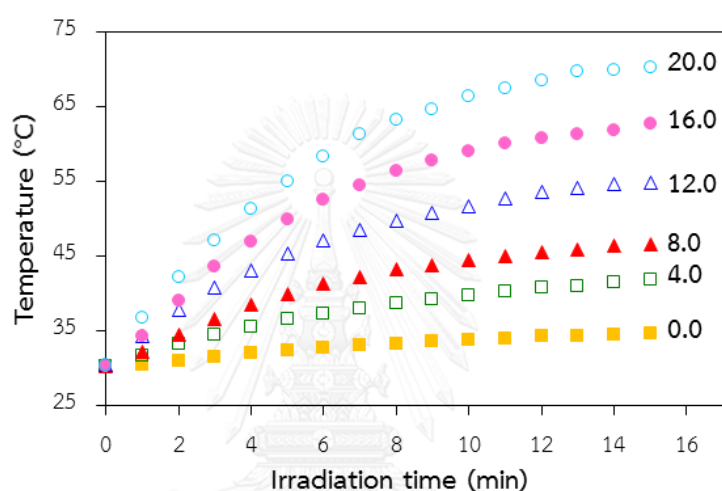


**Figure 3.10** Temperature change of PMAMPC-DOX-AuNRs aqueous solutions having varied quantity of Au element (0 -20  $\mu\text{g}$  in 2 mL of 10mM PBS) during NIR laser irradiation for up to 15 min.

### 3.4 *In vitro* Cytotoxicity Assay

PMAMPC-DOX-AuNRs were evaluated for their cytotoxicity in the presence of live cells. MDA-MB-231 mammary gland adenocarcinoma cells were incubated with CTAB-AuNRs, PMPC-Cys-AuNRs, PMAMPC-DOX-AuNRs and DOX at equivalent concentrations of Au element and DOX for 24 h, followed by cell viability measurements using MTS assay. Dose response curves showed evident cytotoxicity of CTAB-AuNRs (**Figure 3.11**, iv) at a concentration of 2.5  $\mu\text{g}/\text{mL}$ , whereas PMAMPC-Cys-AuNRs (**Figure 3.11**, i) were non-toxic to MDA-MB-231 cells over the entire evaluated concentration range up to the maximum dose tested of 20  $\mu\text{g}/\text{mL}$  indicating that

PMAMPC can truly improve AuNRs biocompatibility. PMAMPC-DOX-AuNRs (Figure 3.11, ii) were tolerated by the cells to a little higher level than DOX (Figure 3.11, iii) indicating that conjugation of DOX with PMAMPC can reduce the toxicity derived from DOX to some extent, with estimated  $IC_{50}$  of 14.6  $\mu\text{g/mL}$  for DOX and  $IC_{50}$  of 17.1  $\mu\text{g/mL}$  for PMAMPC-DOX-AuNRs. From this set of data, the Au element concentration of 5  $\mu\text{g/mL}$  was chosen for the study of synergistic therapy.

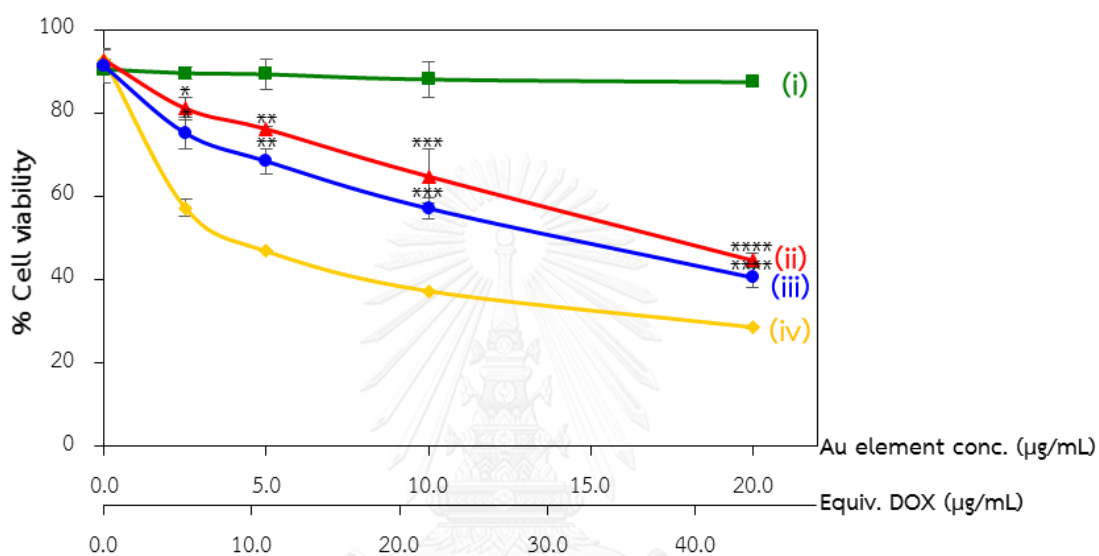


**Figure 3.11** Cell viability (%) of MDA-MB-231 cells after incubation with increasing concentration of compound as determined by MTS assay: (i) PMAMPC-Cys-AuNRs, (ii) PMAMPC-DOX-AuNRs, (iii) DOX and (iv) CTAB-AuNRs. Error bars represent absorbance variability measured at 492 nm where  $n=3$ . \*, \*\*, \*\*\* and \*\*\*\* represent DOX concentration of 5.5, 11.0, 21.9 and 43.8  $\mu\text{g/mL}$ .

### 3.5 Cellular Uptake Study

Due to its self-fluorescent property, intracellular distribution of DOX can be directly followed using confocal laser scanning microscopy (CLSM). Once conjugated with AuNRs, some fluorescence intensity of DOX is particularly quenched as a result of the nanosurface energy transfer (NSET) effect from the AuNRs [13]. After DOX release under acidic environment inside the cells, fluorescence recoveries should be observed.

Therefore, we next examined intracellular localization of in PMAMPC-DOX-AuNRs and acid-triggered DOX release in mammary gland adenocarcinoma (MDA-MB-231) cells using CLSM. MDA-MB-231 cells were incubated with 15  $\mu\text{M}$  DOX with equivalent concentration of the particle for 30 min and 2 h, then counter-stained (in the nucleus) with 4,6-diamidino-2-phenylindole (DAPI), and imaged by CLSM at a set camera exposure time.

As expected, an obvious fluorescent emission of DOX derived from PMAMPC-DOX-AuNRs was observed after just 30 min of incubation (**Figure 3.12**). The extensive red fluorescence of DOX are located inside the cells and only slightly overlapped with blue fluorescence of DAPI-stained nucleus in the overlay image, implying that PMAMPC-DOX-AuNRs were localized in lysosomes and that DOX was released inside lysosomes and partly got into nucleus. With incubation time increased to 2 h (**Figure 3.13**), the greater red fluorescence dots were much more overlapped with the blue fluorescence places DAPI-stained nucleus which can be seen as purple in the overlay image, indicating that pH-triggered DOX release increased with time and increasingly trafficked into nucleus. These findings agreed well with the *in vitro* DOX release results at pH 5.0 using the dialysis method.

In addition, the PMAMPC-DOX alone cannot penetrate the cells within a period of 2 h suggesting that the AuNRs enhanced cell permeability so that PMAMPC-DOX can preferentially accumulate in the cancer cells. Based on these findings above, it can be implied that pH-responsive PMAMPC-DOX-AuNRs not only can reduce the undesired drug release outside the cells during circulation but can also enhance and accelerated the intracellular drug uptake and release, which might enhance the potency of cancer therapy.

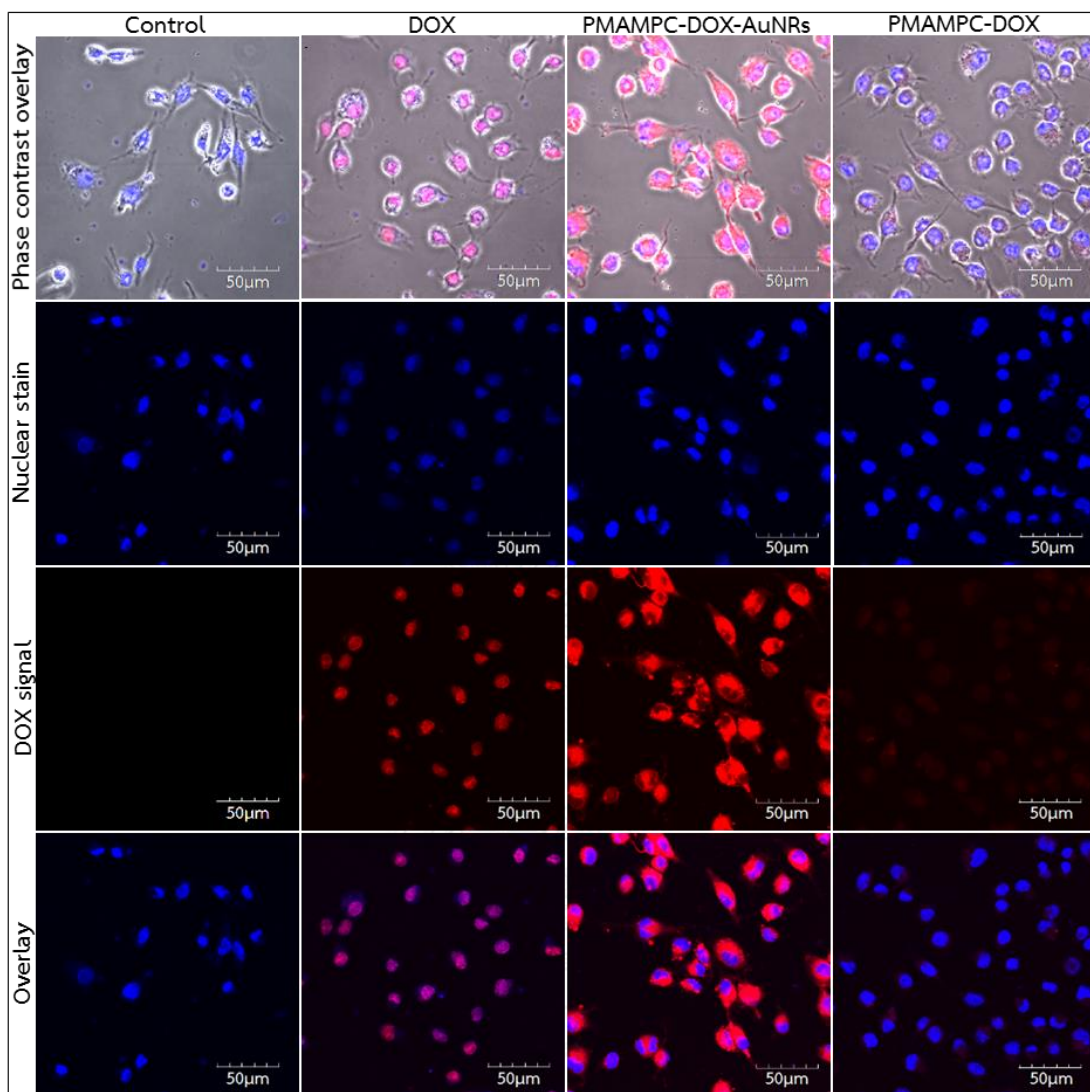


**Figure 3.12** CLSM analysis of intracellular DOX release from PMAMPC-DOX-AuNRs in comparison with DOX and PMAMPC-DOX. MDA-MB-231 cells were treated with PMAMPC-DOX-AuNRs having 15  $\mu\text{g}/\text{mL}$  of DOX for 30 min, followed by CLSM observation with time; blue fluorescence: nucleus staining dry, DAPI; red fluorescence: DOX; scale bar = 50  $\mu\text{m}$ .

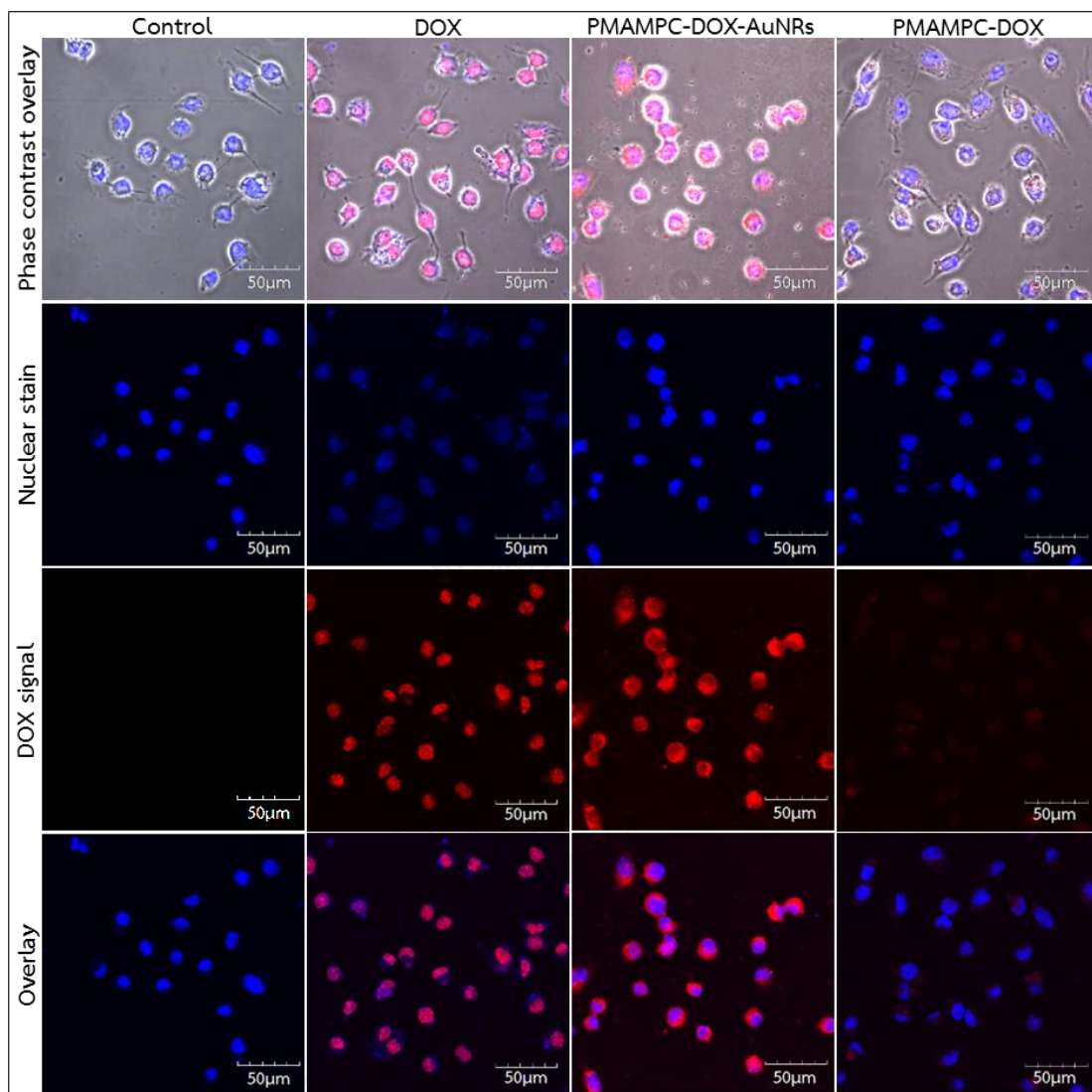


**Figure 3.13** CLSM analysis of intracellular DOX release from PMAMPC-DOX-AuNRs. MDA-MB-231 cells were treated with PMAMPC-DOX-AuNRs having 15  $\mu\text{g}/\text{mL}$  of DOX for 2 h, followed by CLSM observation with time; blue fluorescence: DAPI; red fluorescence: DOX; scale bar: 50  $\mu\text{m}$ .

### 3.6 *In vitro* Synergistic Therapy

The synergistic photothermal-chemotherapy effects of PMAMPC-DOX-AuNRs on MDA-MB-231 cells were also verified using MTS assay. MDA-MB-231 cells were treated with PMAMPC-DOX-AuNRs at a fixed Au element concentration dosage of 5  $\mu\text{g}/\text{mL}$  for

24 h. After laser irradiation for varied period of time (30, 45, and 60 sec), the cells were further cultured in medium for another 24 h. The cell viability was then determined by MTS assay. DOX-free PMAMPC-Cys-AuNRs was used as a control.

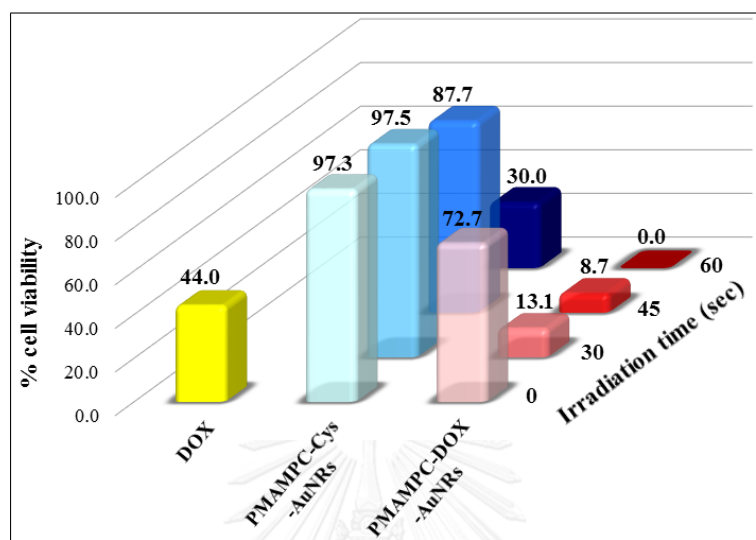


**Figure 3.14** *In vitro* synergistic therapy of PMAMPC-DOX-AuNRs. *In vitro* cytotoxicity of PMAMPC-DOX-AuNRs (blue column), PMAMPC-Cys-AuNRs (red column) and free DOX (yellow column) having Au element concentration = 5  $\mu\text{g}/\text{mL}$  against MDA-MB-231 cells by MTS assay at various irradiation time.

**Figure 3.14** shows that no significant loss of cell viability occurred in PMAMPC-DOX-AuNRs-incubated cells without laser irradiation and DOX-free PMAMPC-Cys-AuNRs-incubated cells after 30 and 45 sec laser irradiation. However, distinctly enhanced cell death was observed for PMAMPC-DOX-AuNRs-treated cells with laser irradiation time of only 30 sec. Photothermal treatment or chemotherapy alone showed no marked cell damage, the synergistic photothermal-chemotherapy was believed to promote the therapeutic effect. The evident reduction of cell viability after combined photothermal-chemo treatment could be explained that DOX released from PMAMPC-DOX-AuNRs weakened the cancer cells and then made them more vulnerable to the heat from photothermal effect resulting in great number of cell death. As irradiation time increased to 60 sec, cells treated with PMAMPC-Cys-AuNRs started to show cell death to a large extent, and cells treated with PMAMPC-DOX-

AuNRs showed complete cell death. Reasonable explanation for the complete cell death of PMAMPC-DOX-AuNRs-treated cells by 60 sec was an additive hyperthermia effect from longer photothermal treatment time resulting in lysosome membrane disruption which led to a fast cell death [13].

This *in vitro* synergistic study demonstrated that the combined photothermal-chemo treatment against cancer cells using PMAMPC-DOX-AuNRs for synergistic hyperthermia ablation and chemotherapy was more effective than either single treatment alone, underlining the great potential of PMAMPC-DOX-AuNRs for cancer treatment.



## CHAPTER IV

### CONCLUSION AND SUGGESTION

PMAMPC having targeted DP of 100 with varied copolymer composition were synthesized by RAFT polymerization. Their molecular weight and copolymer composition were evaluated by  $^1\text{H}$  NMR spectroscopy. Treating the PMAMPC with hydrazine can completely remove dithiobenzoate group and yielded PMAMPC-SH. PMAMPC-SH with 50:50 MA:MPC ratio was chosen to be further modified with cysteamine to introduce additional thiol groups along the chains of copolymer. The resulting PMAMPC-Cys was then reacted with hydrazine to give PMAMPC-Cys-Hy which was subsequently conjugated with DOX by forming hydrazone bonds. The success of stepwise modification and DOX conjugation was verified by FT-IR analysis. %DOX loading was found to be relatively high at 34.3%wt/wt. DOX release from PMAMPC-DOX can apparently be accelerated under acidic condition at pH 5.0 with as high as 86% accumulated release after 48 h as opposed to only 37% of DOX released after the same period of time upon incubation at pH 7.4

CTAB-AuNRs synthesized by seed-mediated growth method exhibited SPR band having a transverse band ( $\lambda_T$ ) and a longitudinal band ( $\lambda_L$ ) at 511 and 800 nm, respectively. As determined by TEM, they were quite uniform in size with  $8.2 \pm 1$  nm in width and  $31.6 \pm 3$  nm in length with aspect ratio  $\sim 3.72$ . Upon ligand exchange of CTAB with PMAMPC-Cys and PMAMPC-DOX, dispersibility of the resulting AuNRs were apparently improved from that of the CTAB-AuNRs due to steric stabilization and hydrophilicity of the copolymer. PMAMPC-DOX-AuNRs were quite uniform in size with  $8.2 \pm 1$  nm in width and  $31.6 \pm 3$  nm in length. The unaltered aspect ratio ( $\sim 3.7$ ) after ligand exchange suggested that polymer coating did not affect the AuNRs morphology. DOX loading content (DLC) of the PMAMPC-DOX-AuNRs was about 19%wt. Photothermal studies verified that the PMAMPC-DOX-AuNRs can convert the absorbed light into heat ( $> 70$  °C) when irradiated with NIR laser at 808 nm for 15 min. Both the



temperature elevation rate and final temperature were correspondingly increased as a function of AuNRs concentration. PMAMPC-DOX-AuNRs were stable under laser irradiation and temperature increase as evidenced from unchanged optical property and size of the particles.

*In vitro* cytotoxicity evaluation by MTS assay suggested that AuNRs was no longer toxic to MDA-MB-231 cells after exchanging CTAB with PMAMPC-Cys over the entire evaluated concentration range up to the maximum dose tested of 20  $\mu\text{g}/\text{mL}$ , indicating that PMAMPC can truly improve AuNRs biocompatibility. PMAMPC-DOX-AuNRs exhibited slightly less toxicity with  $\text{IC}_{50}$  of 17.1  $\mu\text{g}/\text{mL}$  when compared with pure DOX having  $\text{IC}_{50}$  of 14.6  $\mu\text{g}/\text{mL}$ . As monitored by CLSM, PMAMPC-DOX-AuNRs were effectively uptaken into MDA-MB-231 cells and localized in lysosomes. DOX was presumably acid-triggered released inside lysosomes and partly got into nucleus within the first 2 h of incubation. The fact that PMAMPC-DOX alone cannot penetrate the cells suggested that the AuNRs can enhance cell permeability so that PMAMPC-DOX can preferentially accumulate inside the cancer cells. The combined photothermal-chemo treatment of cancer cells using 5  $\mu\text{g}/\text{mL}$  PMAMPC-DOX-AuNRs for synergistic hyperthermia ablation and chemotherapy was more effective than either single treatment alone. Cells were entirely damaged after 60 sec of irradiation. These results suggested that PMAMPC-DOX-AuNRs could potentially be applied in pH-triggered drug delivery for synergistic cancer therapy.

It is our on-going investigation to determine the quantity of DOX uptake inside the cells by flow cytometry. In order to prove whether the DOX release happen as a result of pH-triggered in lysosomes, we planned to use lyso tracker staining method.

## REFERENCES

- [1] Alkilany, A.M.; Thompson, L.B.; Boulos, S.P.; Sisco, P.N., Murphy, C.J. Gold nanorods: Their potential for photothermal therapeutics and drug delivery, tempered by the complexity of their biological interactions *Advanced Drug Delivery Reviews* **2012**, *64*, 190-199.
- [2] Zhang, Z.; Wang, L.; Wang, J.; Jiang, X.; Li, X.; Hu, Z.; Ji, Y.; Wu, X.; Chen, C. Mesoporous silica-coated gold nanorods as a light-mediated multifunctional theranostic platform for cancer treatment *Advanced Materials* **2012**, *24(11)*, 1418-1423.
- [3] Huang, X.; El-Sayed, M.A. Gold nanoparticles: Optical properties and implementations in cancer diagnosis and photothermal therapy *Journal of Advanced Research* **2010**, *1(1)*, 13-28.
- [4] Venkatesan, R.; Pichaimani, A.; Hari, K.; Balasubramanian, P.K.; Kulandaivel, J.; Premkumar, K. Doxorubicin conjugated gold nanorods: a sustained drug delivery carrier for improved anticancer therapy: *Journal of Materials Chemistry B* **2013**, *1(7)*, 1010-1018.
- [5] Xiao, Y.L.; Hong, H.; Matson, V. Z.; Javadi, A.; Xu, W.; Yang, Y. A.; Zhang, Y.; Engle, J. W.; Nickles, R. J.; Cai, W. B.; Steeber, D. A.; Gong, S. Q. Gold nanorods conjugated with doxorubicin and cRGD for combined anticancer drug delivery and PET imaging. *Theranostics* **2012**, *2(8)*, 757-768.
- [6] Chen, C.-C.; Lin, Y.-P.; Wang, C.-W.; Tzeng, H.-C.; Wu, C.-H.; Chen, Y.-C.; Chen, C.-P.; Chen, L.-C.; Wu, Y.-C. DNA-gold nanorod conjugates for remote control of localized gene expression by near infrared irradiation. *Journal of the American Chemical Society* **2006**, *128(11)*, 3709-3715.
- [7] Tree-Udom, T.; et al. Shape effect on particle-lipid bilayer membrane association, cellular uptake, and cytotoxicity. *ACS Applied Materials & Interfaces* **2015**, *7(43)*, 23993-24000.
- [8] Kirui, D.K.; Krishnan, S.; Strickland, A.D.; Batt, C.A. PAA-derived gold nanorods

- for cellular targeting and photothermal therapy. *Macromolecular Bioscience* **2011**, *11(6)*, 779-788.
- [9] Huang, X.H.; El-Sayed, I.H.; Qian, W.; El-Sayed, M.A. Cancer cell imaging and photothermal therapy in the near-infrared region by using gold nanorods. *Journal of the American Chemical Society* **2006**, *128(6)*, 2115-2120.
- [10] Huang, X.; Jain, P.K.; El-Sayed, I.H.; El-Sayed, M.A. Plasmonic photothermal therapy (PPTT) using gold nanoparticles. *Lasers in Medical Science* **2007**, *23(3)*, 217-228.
- [11] Chen, H.; Shao, L.; Li, Q.; Wang, J. Gold nanorods and their plasmonic properties. *Chemical Society Reviews* **2013**, *42(7)*, 2679-2724.
- [12] Liao, H.; Hafner, J.H. Gold Nanorod Bioconjugates. *Chemistry of Materials* **2005**, *17(18)*, 4636-4641.
- [13] Li, X.; Takashima, M.; Yuba, E.; Harada, A.; Kono, K. PEGylated PAMAM dendrimer-doxorubicin conjugate-hybridized gold nanorod for combined photothermal-chemotherapy. *Biomaterials* **2014**, *35(24)*, 6576-6584.
- [14] Chen, X.J.; Parelkar, S.S.; Henchey, E.; Schneider, S.; Emrick, T. PolyMPC-doxorubicin prodrugs. *Bioconjugate Chemistry* **2012**, *23(9)*, 1753-1763.
- [15] Du, J.-Z.; Du, X.-J.; Mao, C.-Q.; Wang, J. Tailor-made dual pH-sensitive polymer-doxorubicin nanoparticles for efficient anticancer drug delivery. *Journal of the American Chemical Society* **2011**, *133(44)*, 17560-17563.
- [16] Iwasaki, Y.; Ishihara, K. Cell membrane-inspired phospholipid polymers for developing medical devices with excellent biointerfaces. *Science and Technology of Advanced Materials* **2012**, *13(6)*, 064101.
- [17] Akkhat, P.; Kiatkamjornwong, S.; Yusa, S.-i.; Hoven, V.P.; Iwasaki, Y. Development of a novel antifouling platform for biosensing probe immobilization from methacryloyloxyethyl phosphorylcholine-containing copolymer brushes. *Langmuir* **2012**, *28(13)*, 5872-5881.
- [18] Chen, X.J.; Lawrence, J.; Parelkar, S.; Emrick, T. Novel zwitterionic copolymers

- with dihydrolipoic acid: Synthesis and preparation of nonfouling nanorods. *Macromolecules* **2013**, *46*(1), 119-127.
- [19] Page, S.M.; Henchey, E.; Chen, X.J.; Schneider, S.; Emrick, T. Efficacy of polyMPC-DOX prodrugs in 4T1 tumor-bearing mice. *Molecular Pharmaceutics* **2014**, *11*(5), 1715-1720.
- [20] Moad, G.; et al. Living free radical polymerization with reversible addition-fragmentation chain transfer (the life of RAFT). *Polymer International* **2000**, *49*(9), 993-1001.





APPENDIX

จุฬาลงกรณ์มหาวิทยาลัย  
CHULALONGKORN UNIVERSITY

Calculation of copolymer composition and degree of polymerization using  $^1\text{H}$  NMR integration.

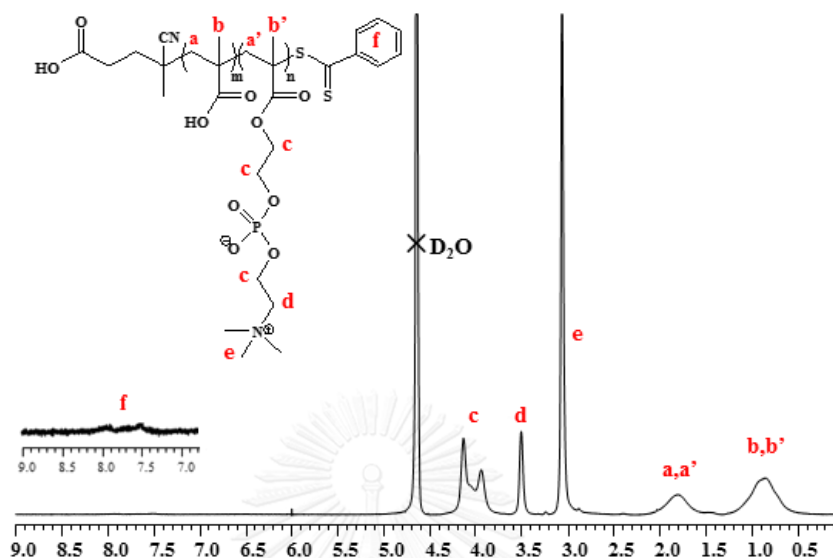


**Figure A1**  $^1\text{H}$  NMR spectrum of PMAMPC in  $\text{D}_2\text{O}$

The copolymer composition (MA:MPC) determined from  $^1\text{H}$ -NMR spectra (**Figure A1**) by integrating peak b,b' at  $\delta$  0.9 ppm ( $\text{CH}_3$  proton of both MPC and MA) and peak d at  $\delta$  3.5 ppm ( $\text{CH}_2$  protons of MPC) against peak f at around 7.4-8.2 ppm (protons of aromatic) as shown in equation A1-5.

$$\text{Total unit} = \frac{f_{b,b'}}{2} / \frac{f_f}{5} \quad (\text{A1})$$

$$\text{MPC unit} = \left[ \frac{f_d}{6} / \frac{f_f}{5} \right] \times 2 \quad (\text{A2})$$

$$\text{MA unit} = \text{Total unit} - \text{MPC unit} \quad (\text{A3})$$

$$\% \text{ MPC} = \frac{\text{MPC unit}}{\text{Total unit}} \times 100 \quad (\text{A4})$$

$$\% \text{ MA} = \frac{\text{MA unit}}{\text{Total unit}} \times 100 \quad (\text{A5})$$

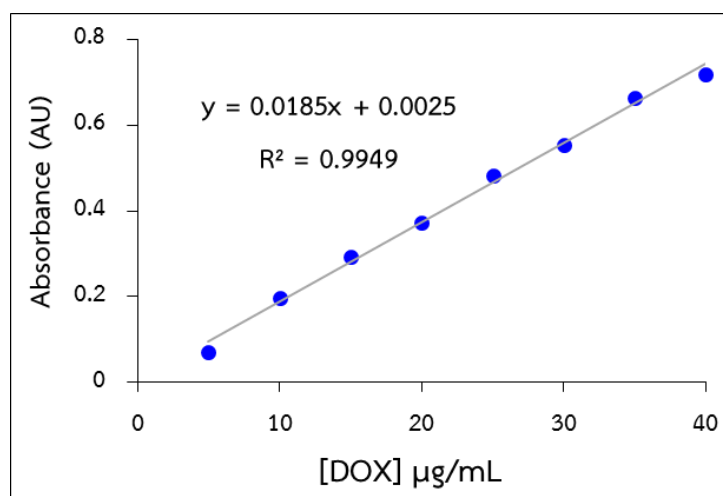


Figure A2 DOX calibration curve measured in Milli-Q water.



## VITA

Miss Phim-on Khunsuk was born on January 23rd, 1991 in Anghong, Thailand. She graduated a Bachelor degree of Science, majoring in Chemistry from Kasetsart University in 2013. In the same year, she was admitted to the Master's degree of Science, program in Organic Chemistry, at Chulalongkorn University and graduated in the academic year of 2015.

### International Publication:

1. Phim-on Khunsuk, Voravee P. Hoven "Development of Gold Nanorods Stabilized with Drug-conjugated Polymer for Synergistic Cancer Therapy" Proceedings of Pure and Applied Chemistry International Conference 2016, BITEC, Bangkok, Thailand, February 9-11, 2016, pp 962-967.